

Development of a plant carbon-nitrogen interface coupling framework in a coupled biophysical-ecosystem-biogeochemical model (SSiB5/Triffid/DayCent-SOM v1.0): Its parameterization, implementation, and evaluation

5

Zheng Xiang^{1,2}, Yongkang Xue^{2*}, Weidong Guo^{1,4*}, Melannie D. Hartman³, Ye Liu^{2,5}, William J. Parton³

¹School of Atmospheric Sciences, Nanjing University, Nanjing, China

²Department of Geography, University of California, Los Angeles, CA 90095, USA

³Natural Resource Ecology Laboratory, Colorado State University, CO 80523, USA

10 ⁴Joint International Research Laboratory of Atmospheric and Earth System Sciences, Nanjing, China

⁵Pacific Northwest National Laboratory, Richland, WA 99352, USA.

Correspondence to: Yongkang Xue (yxue@geog.ucla.edu), Weidong Guo (guowd@nju.edu.cn)

15 **Abstract.** Plant and microbial nitrogen (N) dynamics and N availability regulate the photosynthetic capacity and capture, allocation, and turnover of carbon (C) in terrestrial ecosystems. Studies have shown that a wide divergence in representations of N dynamics in land surface models leads to large uncertainty in the biogeochemical cycle of the terrestrial ecosystems and then in climate simulations as well as the projections of future trajectories. In this study, a plant C-N interface coupling framework is developed and implemented in a coupled biophysical-ecosystem-biogeochemical model (SSiB5/TRIFFID/
20 DayCent-SOM v1.0). The main concept and structure of this plant C-N framework and its coupling strategy are presented. This framework takes more plant N-related metabolism processes into account. For instance, plant resistance and self-adjustment is represented by a dynamic C/N ratio for each plant functional type (PFT). Furthermore, when available N is less than plant N demand, plant growth is restricted by a lower maximum carboxylation capacity of Rubisco (V_{max}) level, reducing gross primary productivity (GPP). In addition, a module for plant respiration rates is introduced by adjusting the respiration
25 with different rates at different plant components for the same N concentration. Since insufficient N can potentially give rise to lags on plant phenology, phenology scheme is also adjusted with a lag factor related to N processes. All these considerations ensure a more comprehensive incorporation of N regulations to plant growth and C cycling. This new approach has been tested systematically to assess the effects of this coupling framework and N limitation on the terrestrial carbon cycle. Long term measurements from both flux tower sites with different PFTs and global satellite-derived products are employed as references
30 to assess these effects. The results show a general improvement with the new plant C-N coupling framework, with more



consistent emergent properties, such as GPP and leaf area index (LAI), compared to observations. The main improvements occur in tropical Africa and boreal regions, accompanied by a decrease of the bias in global GPP and LAI by 16.3% and 27.1%, respectively.

1 Introduction

35 Land surface processes substantially affect climate (Foley et al., 1998; Ma et al., 2013; Sellers et al., 1986; Xue et al., 2004, 2010, 2022, 2023) and are influenced by climate in turn (Bonan, 2008; Liu et al., 2019, 2020; Zhang et al., 2015), forming complex feedback loops to climate change (Friedlingstein et al., 2006; Gregory et al., 2009). To study these processes, the land surface components of Earth System Models (ESMs) have evolved from those that only represent biophysical processes (i.e., hydrology and energy cycle) to those that include the terrestrial carbon (C) cycle, vegetation dynamics, and nutrient processes
40 (Cox, 2001; Dan et al., 2020; Foley et al., 1998; Jiang et al., 2014; Niu et al., 2020; Oleson et al., 2013; Pan et al., 2017; Sellers et al., 1986; Sitch et al., 2003; Wang et al., 2010; Yang et al., 2019; Zhan et al., 2003).

Current land surface models have large uncertainties in predicting historical and recent C exchanges (Beer et al., 2010; Richardson et al., 2012; Zaehle et al., 2015). The parameterization of some processes has been criticized for being oversimplified from an ecological point of view (Ali et al., 2015; Lawrence et al., 2019; Reich et al., 2006), and the dynamic
45 vegetation models tend to overestimate terrestrial C sequestration (Anav et al., 2015; Murray-Tortarolo et al., 2013; Mueller et al., 2019; Gristina et al., 2020; Oliveira et al., 2021; Heikkinen et al., 2021). The uncertainty/errors in predictions using land models have been attributed to many factors. The inclusion or exclusion of nutrient limitations on productivity is one of the critical factors. Those C-only models ignore significant nitrogen (N) impacts and therefore overestimate C sequestration by terrestrial ecosystems under climate change (Peñuelas et al., 2013; Zaehle et al., 2015). Ecosystem N cycling processes are
50 among the dominant drivers of terrestrial C-climate interactions through their impacts, mainly N limitation, on vegetation growth and productivity (Reich et al., 2006), especially in N-poor younger soils at high latitudes (LeBauer & Treseder, 2008; Vitousek and Howarth, 1991), and on microbial decomposition of organic matter (Hu et al., 2001). As such, the N cycle and its effect on C uptake in the terrestrial biosphere has been incorporated in land surface models (LSMs) of ESMs (Davies-Barnard et al., 2020) with various representations of N processes (Ali et al., 2015; Asaadi et al., 2021; Best et al., 2011; Clark
55 et al., 2011; Davies-Barnard et al., 2020; Ghimire et al., 2016; Goll et al., 2017; Krinner et al., 2005; Lawrence et al., 2019; Matson et al., 2002; Oleson et al., 2013; Smith et al., 2014; Thum et al., 2019; Wang et al., 2010; Wiltshire et al., 2020; Yu et al., 2020; Zhu et al., 2019).

In the latest Coupled Model Intercomparison Project Phase 6 (CMIP6, Eyring et al., 2016), although there were 112 different coupled models with various land surface models from 33 research teams, only about 10 models incorporated an N cycle
60 module (Arora et al., 2020). The coupling of N processes is still an area of model development. Among these models including N processes, most of them pay more attention to microbial N dynamics in soil. The adequate C-N coupling in plant N processes has been indicated as an area that still needs intensive investigation (Thum et al., 2019; Ghimire et al., 2016; Goll et al., 2017;



Yu et al., 2020; Zaehle et al., 2015; Zhu et al., 2019). Some key plant N processes, such as N limitation on GPP, the effect of biomass N content on autotrophic respiration, plant N uptake, ecosystem N loss, and biological N fixation, have been introduced into LSMs with various complexity to present the N limitation effects in current land models. They include, for instance, using N to scale down the photosynthesis parameter $V_{c,max}$ (Ghimire et al., 2016; Zaehle et al., 2015) or potential GPP to reflect N availability (Gerber et al., 2010; Oleson et al., 2013; Wang et al., 2010); defining a C cost of N uptake (Fisher et al., 2010) and optimizing N allocation for leaf processes (Ali et al., 2015). In many of these approaches, N limitation is represented as instantaneous down-regulation of potential photosynthesis rates based on soil mineral N availability.

This paper presents a recently developed process-based approach, which mainly focuses on the N limitation effects and plant resistance on photosynthesis, plant respiration, and plant phenology. The dynamic plant C/N ratio is a key concept in representing plant resistance, self-adjustment, and C/N interactions. Due to their relative immobility, plants often face significant challenges in obtaining an adequate supply of nutrients to meet the demands of basic cellular processes. A deficiency of any type of nutrient may result in decreased plant productivity and/or fertility (McDowell et al., 2008; Morgan and Connolly, 2013; Stenberg and Muola, 2017). Evidence has shown that plant C/N ratios have to change over the plant's lifecycle with nutrient availability (Chen and Chen, 2021; McGroddy et al., 2004; Meyer-Grünefeldt et al., 2015; Sardans et al., 2012; Smith, 1991; Yang et al., 2021; Zhang et al., 2011) through plant self-adjustment. Plant cells C/N ratios are influenced by the accumulation of C polymers, such as carbohydrates and lipids, and are greater when cells are nutrient starved, or exposed to high light (Aber et al., 2003; MacDonald et al., 2002; Talmy et al., 2014). However, many land models specify fixed plant C/N ratios for each plant functional type (PFT) (e.g., Best et al., 2011; Clark et al., 2011; Krinner et al., 2005; Oleson et al., 2013; Wang et al., 2010). In this paper, we present a new plant C-N coupling framework with flexible C/N ratios (Section 2.2.2), in which N regulates photosynthesis (Section 2.2.3), respiration (Section 2.2.4), and plant phenology (Section 2.2.5), as well as produces a consistent coupling between biophysical and biogeochemical processes. Allometric relations and empirical data sets are used to constrain the range of possible C/N ratios. This dynamic C/N ratio depends on the degree to which the N demands of different plant organs (e.g., leaf, root, and wood) are satisfied over the past several days. This plant C-N framework takes some plant N metabolism processes into account and prevents unrealistic instantaneous down-regulation of potential photosynthesis rates.

We implement this plant C-N framework by coupling a soil organic matter and nutrient cycling model (DayCent-SOM, Del Grosso et al., 2000; Parton et al., 1998, 2010) with a biophysical/dynamic vegetation model (SSiB5/TRIFFID, the Simplified Simple Biosphere Model version 5/ Top-down Representation of Interactive Foliage and Flora Including Dynamics Model, Cox, 2001; Harper et al., 2016; Liu et al., 2019; Xue et al., 1991; Zhan et al., 2003; Zhang et al., 2015). DayCent-SOM, which includes only the soil organic matter (SOM) cycling and trace gas subroutines from the DayCent ecosystem model (Parton et al., 1998, 2010) represents SOM transformations, below-ground N cycling, soil N limitation to microbial processes and plant growth, and nitrification/denitrification processes. In the coupled model, the potential N uptake depends on plant N demand from a biophysical and dynamic vegetation model, SSiB5/TRIFFID. The actual plant N uptake is limited based on soil N availability as predicted by DayCent-SOM (Del Grosso et al., 2000; Parton et al., 1998; 2010). The coupled model is verified



at twelve flux tower sites with different PFTs and is used to conduct several sets of global 2-D offline simulations from 1948 to 2007 to assess the effects of the coupling process. The model predictions of global GPP and LAI are evaluated against satellite-derived observational data. The results demonstrate the relative importance of different plant N processes in this C-N framework.

The model used in this paper is presented in section 2.1. The development and implementation of this plant C-N framework is presented in section 2.2. The model forcing and validation data used in this paper are presented in section 2.3. In section 3, the experimental design is described. In section 4, the measurements from the flux tower sites with different PFTs and the global satellite-derived observations from 1948-2007 are used as references to assess the effect of the C-N coupling process on the long-term mean vegetation distribution and terrestrial C cycling using the offline SSiB5/TRIFFID/DayCent-SOM. Some issues and conclusions are presented in section 5.

2 Methods

2.1 Model description

2.1.1 SSiB4/TRIFFID model

The Simplified Simple Biosphere Model (SSiB, Xue et al., 1991; Sun and Xue, 2001; Zhan et al., 2003) is a biophysical model that simulates fluxes of surface radiation, momentum, sensible/latent heat, runoff, soil moisture and temperature, and vegetation GPP based on energy and water balance and photosynthesis processes. The SSiB was coupled with a dynamic vegetation model, the Top-down Representation of Interactive Foliage and Flora Including Dynamics Model (TRIFFID), to calculate NPP, LAI, canopy height, and PFT fractional coverage according to the C balance (Cox, 2001; Harper et al., 2016; Liu et al., 2019; Zhang et al., 2015). Moreover, the surface albedo and aerodynamic resistances are also updated based on the vegetation conditions. Previous work has improved the PFT competition strategy and plant physiology processes to make the SSiB4/TRIFFID suitable for seasonal, interannual, and decadal studies (Zhang et al., 2015). SSiB4/TRIFFID includes seven PFTs: (1) broadleaf evergreen trees (BET), (2) needleleaf evergreen trees (NET), (3) broadleaf deciduous trees (BDT), (4) C3 grasses, (5) C4 plants, (6) shrubs, and (7) tundra. PFT coverage is determined by net C availability, competition between species, and disturbance, which includes mortality due to fires, pests, and windthrow. A detailed description and validation of SSiB4/TRIFFID can be found in Zhang et al. (2015), Liu et al. (2019), and Huang et al. (2020). In this study, The DayCent-SOM (see next section) is introduced and coupled with the SSiB5/TRIFFID using the C-N interface coupling framework introduced in this study, which will be discussed in Section 2.2.

2.1.2 DayCent-SOM model

DayCent-SOM, a subset of DayCent that excludes plant growth, soil hydrology, and soil temperature subroutines, consists of soil mineral N pools (ammonium and nitrate) and six types of organic C and N pools consisting of two non-woody plant litter

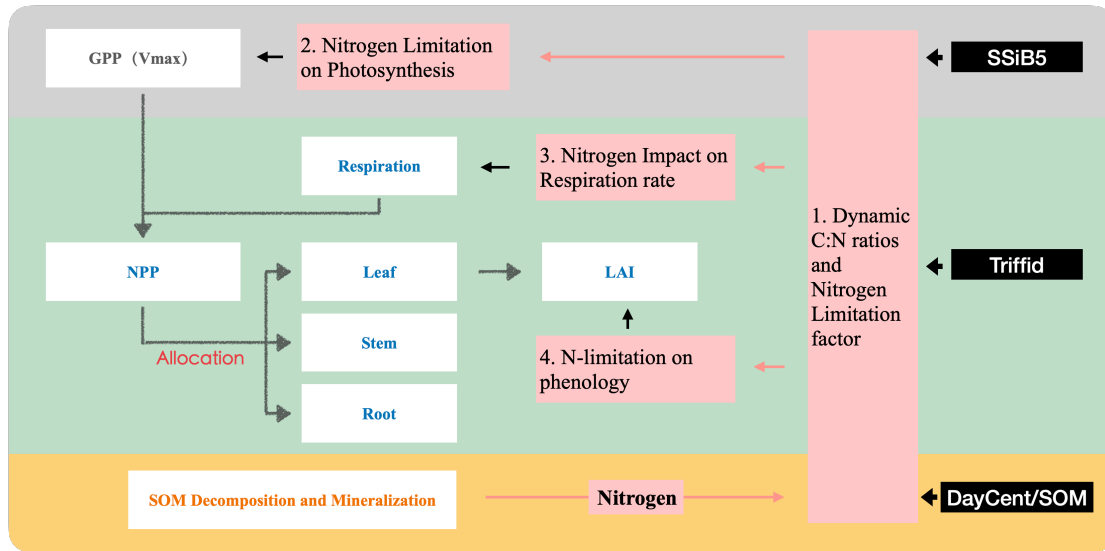


130 pools (metabolic and structural), three coarse woody debris pools (from death of large wood, fine branches, and coarse roots),
and three kinetically defined organic matter pools, (active, slow, and passive); all types of organic pools except the passive
pool have both above-ground and below-ground counterparts. Non-woody plant litter is partitioned into structural (lignin +
cellulose) and metabolic (labile) litter based on the lignin: N ratio of plant material (Parton et al., 1994)). The coarse woody
debris pools decay in the same way that the structural pool decomposes, with lignin and cellulose going to the slow soil organic
matter pool and the labile fraction going to the active soil organic matter pool. Each type of organic pool has its own intrinsic
rate of decomposition, modified by temperature and moisture effects (Parton et al., 1994). Additionally, the decomposition
rates of the structural material and coarse woody debris pools are functions of their respective lignin fractions. DayCent's litter
135 decay model has been validated using extensive data from the LIDET litter decay experiments from all over the world (Bonan
et al., 2013)

2.2 Development of a plant Carbon-Nitrogen (C-N) Interface coupling framework

2.2.1 Conceptual considerations and coupling strategy

To represent C/N interactions, we have developed a plant C-N interface framework to take into account both biophysical and
140 biochemical C/N processes in plant life activities. In this study, we applied the coupling framework to SSiB5/TRIFFID/
DayCent-SOM. However, this approach could be applied to any other process-based models with similar physical/biological
principles. The conceptual considerations in developing this framework are presented in this section. For a process-based
model, introducing a consistent coupling philosophy between biophysical and biogeochemical processes is necessary. The soil
N dynamics model (DayCent-SOM) is directly driven by soil temperature/moisture as well as plant C/N litter inputs into soil.
145 Because the surface water, radiation, and carbon fluxes and plant litter are calculated by SSiB5, we force DayCent-SOM with
SSiB5-produced soil temperature, soil moisture, and SSiB5/TRIFFID-produced plant litter. DayCent-SOM then computes
daily changes of all organic matter and mineral soil pools, estimates losses of N from nitrate leaching and N₂O, NO_x, and N₂
emissions, predicts the amount of inorganic N available to plants, and updates inorganic N pools after accounting for plant N
uptake by SSiB5. Following plant N uptake from DayCent-SOM, our plant C-N interface framework describes N effects on
150 plant physiology from photosynthesis, plant autotrophic respiration, and plant phenology plus a dynamic C/N ratio (Fig. 1).
Following such model development philosophy, our framework not only considers N limitation on the general plant
photosynthesis process but also emphasizes the N limitation effect during the growth season, which can represent the
physiological processes of C-N cycling and help us obtain more information to understand the attribution of N processes on
the C cycle.



155

Figure 1. Schematic diagram of plant biogeochemistry and nitrogen impacts in SSiB5/TRIFFID/DayCent-SOM.

Notes: (1) Different background color represents three different modules: SSiB, TRIFFID, and DayCent/SOM; (2) White boxes indicate the main processes in C-N coupling in different modules; (3) Vermeil boxes indicate how nitrogen influences plant biogeochemistry through the C-N framework.

160

In the original land surface model (SSiB4/TRIFFID), with assumed unlimited N availability and fixed C/N ratios based on PFT, the assimilated C determined the N contents of leaf, stem, and root, which influenced autotrophic respiration, followed by GPP, LAI, and NPP. However, more evidence indicates the C/N ratio is not fixed in plant life. The studies of Ecological Stoichiometry (Sterner and Elser, 2002), which investigates how the availability of multiple elements, including carbon, nitrogen, and phosphorus, constrain ecological interactions, reveals that plants can adjust their resource requirements. Changes in N resource availability will result in changes to plant C allocation and partitioning. Studies show that plants resorb only about 50% of leaf N on average (Aerts, 1996) to conserve nutrients (Clarkson and Hanson, 1980) and to increase nutrient use efficiency (Herbert & Fownes, 1999; Vitousek, 1982). These processes cause a major internal nutrient flux and changes of C/N ratios to reduce the impact of N limitation (Talhelm et al., 2011; Vicca et al., 2012). In addition, plant responses, such as plant resistance and self-adjustment, will be limited under fixed C/N ratios, which affect plant productivity and litter N content, thus driving changes in the underground biogeochemistry and ultimately C and N uptake and storage (Drewniak and Gonzalez-Meler, 2017). Some studies show that the increase in foliar N under increased soil N availability would improve plant responses because it allows adaptations in the stoichiometry of C and N (Bai et al., 2021; Chang et al., 2022; Ding et al., 2022; Kaiser et al., 2014; Lin et al., 2022; Zhang et al., 2022). The main impact will be to decrease C/N ratio in leaves when the available N increases, driving increases in productivity and changes in soil and litter N content (Drewniak and Gonzalez-Meler, 2017). A dynamic C/N ratio is employed in our framework to obtain N states more realistically and properly represent the effect of N processes (See section 2.2.2 for more details).

170

175



A commonly used parameterization of photosynthetic C assimilation by the terrestrial biosphere in ESMs is represented by the
180 Farquhar, von Caemmerer, and Berry (FvCB) model of photosynthesis (Collatz et al., 1991; Farquhar et al., 1980). Plants
require N as essential components of photosynthetic proteins involved in light capture, electron transport, and carboxylation
(Evans, 1989). Nitrogen is an important constituent of the Rubisco enzyme and mitochondrial enzymes that regulate respiration
and adenosine triphosphate (ATP) generation (Makino and Osmond, 1991). One of the most important photosynthetic model
parameters, the maximum carboxylation rate by the Rubisco enzyme ($V_{c,max}$) is a key parameter in the FvCB model (Farquhar
185 et al., 1980) and has an extensive range across the models depending on the plant N content (Rogers, 2014). Since N is an
important component of the Rubisco enzyme, leaf N content will affect $V_{c,max}$ and thus GPP. The original FvCB model did
not explicitly consider the N effect on photosynthesis. In a number of LSMs, an empirical relationship is applied to relate
 $V_{c,max}$ to leaf N content N_{leaf} to generate the effect of N on photosynthesis, e.g., $V_{c,max} = i_v + s_v \times N_{leaf}$, where the intercept
(i_v) and slope (s_v) are derived for each PFT based on observations (Kattge et al., 2009; Raddatz et al., 2007). Moreover, in
190 some coupling approaches, only the relationship between the root N uptake and GPP/NPP is considered to represent the N
limitation on C cycles (Ali et al., 2015; Fisher et al., 2010; Ghimire et al., 2016). However, because NPP is the difference
between GPP and autotrophic respiration, adjusting NPP or GPP alone may cause the ratio between NPP and respiration to
deviate from reality. Using the process-based N limitation factor produced from DayCent-SOM to modify $V_{c,max}$ (See section
2.2.3) is a more realistic way to produce the N effect on the photosynthesis process. Moreover, when calculating the N limit
195 to Rubisco capacity, an aforementioned dynamic C/N ratio is introduced in our approach to influence the N-limit effect on
photosynthesis.

Nitrogen is not only a dominant regulator of vegetation dynamics, GPP, NPP, and terrestrial C cycles; Reich et al., (2008)
demonstrate strong relationships between respiration and N limitation based on observational data from various species. At
any normal N concentration, respiration rates are consistently lower on average in leaves than in stems or roots. Therefore, we
200 introduce two parameters for stems and roots, respectively, based on PFT to adjust the respiration rate in section 2.2.4.

Nitrogen also affects plant phenology and can be remobilized to supply spring bud-break or vegetative shoot extension (Kolb
and Evans, 2002; Marmann et al., 1997; Millard, 1994; Neilsen et al., 1997). Nitrogen resorption is found during leaf
senescence and growth in evergreens (May and Killingbeck, 1992). Because plants need time to turnover, the plant N processes
also have a lag effect on plant phenology (Thomas et al., 2015). Phenology in SSiB4/TRIFFID modulates LAI evolution,
205 including leaf mortality, but it is not directly linked to N. Since different N states and supplements will lead to different lags
on phenology, we add N impact on plant phenology by introducing a N limitation parameter, which will be discussed in section
2.2.5.

2.2.2 Dynamic C/N ratio based on plant growth and soil nitrogen storage

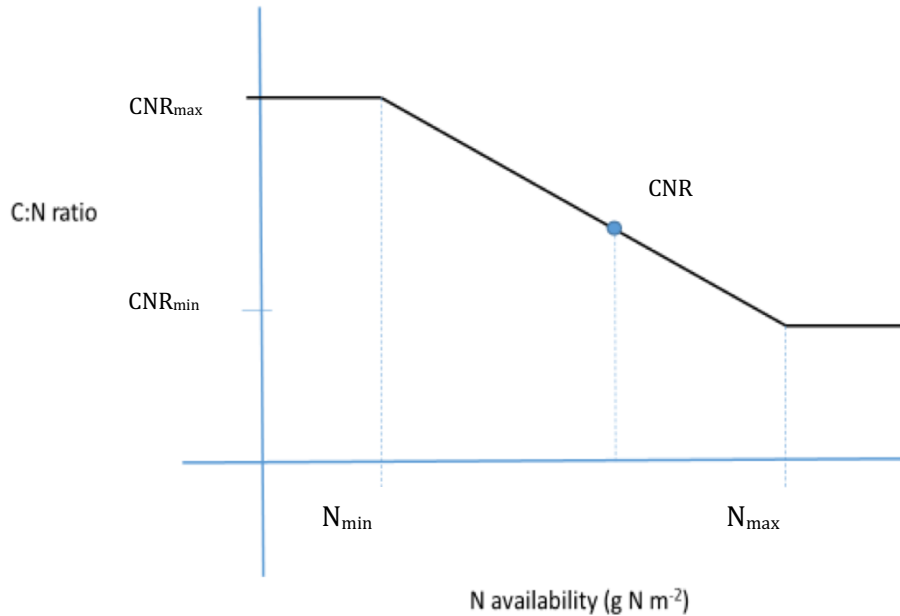
Plant resistance and self-adjustment to N availability (N_{avail}) are represented by dynamic C/N ratios (CNRs) in SSiB5. The N
210 availability for new growth limits the C assimilation rate through the CNRs, i.e., the model simulated NPP should be no more



than $N_{avail} \times CNR$ of new plant material. In the original TRIFFID parameterization, the CNRs for different plant components (leaf, root, and wood) are fixed based on plant functional types (Cox, 2001); and changes in CNR occurred over the lifecycle of the plant, varied with nutrient availability, and were not considered in the original SSiB4/TRIFFID models. A linear relationship between CNR and N_{avail} , based on the DayCent's parameterization, is introduced to the
 215 SSiB5/TRIFFID/DayCent-SOM for each PFT's components, (Fig. 2, Eq. 1).

$$CNR = \begin{cases} CNR_{max}, & N_{avail} \leq N_{min} \\ \frac{N_{avail} - N_{max}}{N_{min} - N_{max}} \times CNR_{min} + \frac{N_{avail} - N_{min}}{N_{max} - N_{min}} \times CNR_{max}, & N_{min} < N_{avail} < N_{max} \\ CNR_{min}, & N_{avail} \geq N_{max} \end{cases} \quad (1)$$

where N_{avail} is the amount of soil mineral nitrogen that was available at the end of the previous day (g N m^{-2}) calculated from DayCent-SOM.



220 **Figure 2.** The relationship between soil nitrogen availability and plant carbon-nitrogen ratios.

The minimum and maximum amounts of nitrogen (N_{min} , N_{max}) necessary for the potential NPP_p ($\text{g C m}^{-2} \text{ day}^{-1}$), which is first calculated from the SSiB4/TRIFFID with unlimited N, are:

$$N_{min} = \frac{NPP_p}{CNR_{max}} \quad (2)$$

225
$$N_{max} = \frac{NPP_p}{CNR_{min}} \quad (3)$$

where CNR_{min} and CNR_{max} are the minimum and the maximum C/N ratio for each PFT's components from the DayCent (Table 1). The CNR ranges of leaves, fine roots, and stems/wood are from DayCent's user's manual and other published papers



(Parton et al., 1993, 2007). Please note that Eq. (2) and Eq. (3) are calculated based on potential NPP; the CNR that is calculated based on Eqs. 1-3 ensures that when N_{avail} varies between N_{min} and N_{max} , the plant can adjust CNR to support this potential NPP (as demonstrated in the schematic diagram Figure 2). That said, the N limitation will have no effect on the C assimilation as long as N_{avail} is larger than N_{min} . However, the N content of plant litter falling to the soil was determined by this dynamic C/N ratio. Compared with the constant CNR, the range of possible plant carbon variation with dynamic CNR is smaller, reducing the impact of N limitation. As reviewed in the introduction and previous section, a number of recent studies have demonstrated that allowing adaptations in the stoichiometry of C and N would improve plant responses; for instance, an increase in available foliar N decreases the C/N ratio in leaves, driving an increase in productivity.

Table 1. C:N ranges of leaves, fine roots, and stems/wood for each plant function type (PFT).

	Plant component	CNR_{min}	CNR_{max}
Broadleaf deciduous	leaves	20	50
	roots	40	70
	wood	200	500
Broadleaf Evergreen	leaves	20	40
	roots	40	70
	wood	150	300
Needleleaf Evergreen	leaves	30	60
	roots	40	60
	wood	400	800
C3 grass	leaves	20	40
	roots	40	50
	wood	40	80
C4 grass	leaves	20	60
	roots	60	100
	wood	60	100
shrub	leaves	20	40
	roots	40	70
	wood	200	400
tundra shrub	leaves	20	40
	roots	40	80
	wood	300	700

Note: Data of CNR_{min} and CNR_{max} for each PFT's components are from DayCent's user's manual and other publications (Parton et al., 1993, 2007)



The DayCent-SOM only provides the total available nitrogen (N_{avail}) for the plant within one grid box, which consists of several PFTs. To apply equation 1, the nitrogen available for each PFT and its plant components in the grid box is calculated as

$$245 \quad N_{avail}(i) = N_{avail} * frac_i \quad (4)$$

$$N_{avail}(i,j) = N_{avail}(i) * \Delta C_j / \sum_j \Delta C_j \quad (5)$$

where $frac_i$ is the fraction of PFT i in one grid, and ΔC_j is the fraction of carbon allocated to plant component j , which consists of leaf, root, and wood, and is calculated in TRIFFID.

2.2.3 Effect of nitrogen limitation on photosynthesis based on soil available nitrogen and plant C-N ratio

250 There are several different ways to represent N limitation effects in land models, including using N to scale down photosynthesis (Ghimire et al., 2016; Goll et al., 2017; Thum et al., 2019; Yu et al., 2020; Zaehle et al., 2015; Zhu et al., 2019), scaling down potential GPP based on N availability (Gerber et al., 2010; Oleson et al., 2013; Wang et al., 2010), or defining an NPP cost of nitrogen uptake (Fisher et al., 2010). We choose the most physiological way by adjusting maximum Rubisco carboxylation rate ($V_{c,max}$) during the photosynthesis process, rather than adjusting NPP at the end of the photosynthesis
255 process. $V_{c,max}$ regulates both C assimilation and autotrophic respiration; and the photosynthesis assimilation product, GPP, is proportional to $V_{c,max}$, which is proportional to nitrogen content of the Rubisco leaf reserves.

We therefore introduce a downregulation of the canopy photosynthetic rate based on the available mineral N for new growth (N_{avail}) using a N-availability factor, $f(N)$.

$$V_{c,max,Nlimit} = V_{c,max} * f(N) \quad (6)$$

260 The $f(N)$ is determined by nitrogen availability:

$$f(N) = \begin{cases} \frac{N_{avail}}{N_{min}} & N_{avail} \leq N_{min} \\ 1 & otherwise \end{cases} \quad (7)$$

Because plants can adjust the relative allocations of C and N during N uptake via N remobilization and resorption to reduce the impact of N limitation, as discussed in the previous section for dynamic CNR, the N-limit effect on photosynthesis only applies when nitrogen availability is lower than the minimum amounts of nitrogen (N_{min}) necessary for the potential NPP.

265 We take into account that plants have resistance and self-adjustment through this approach to make the N-limit effect neither linearly nor instantaneously responsive to available N content. A linear relationship between $f(N)$ and N_{avail} is valid only when N availability is not sufficient for the minimum N demand for new growth.

In fact, the factor, $f(N)$ can also be applied to NPP and GPP as shown in Equations 8a –b.

$$NPP_{Nlimit} = NPP * f(N) \quad (8a)$$

$$270 \quad GPP_{Nlimit} = GPP * f(N) \quad (8b)$$

If NPP is adjusted (Eq. 8a), this means the same N limitation for photosynthesis is applied for plant respiration, which is not reasonable based on plant physiology (Högberg et al., 2017). Such approach may distort the ratio of NPP and respiration. If



only GPP is adjusted for N-limitation, then the N limitation for respiration is ignored. Therefore, we choose an approach to adjust $V_{c,max}$, which is related to N during the photosynthesis process and affects both C uptake and autotrophic respiration.

275 2.2.4 Improvement of nitrogen impact on respiration rates based on field observations

Nitrogen affects plant respiration (Reich et al., 2008; Thornely and Johnson, 1990). In the original SSiB4/TRIFFID, the total maintenance respiration (R_{pm}) is given by Cox (2001):

$$R_{pm} = 0.012R_{dc} \frac{N_l + N_s + N_r}{N_l} \quad (9)$$

where R_{dc} is canopy dark respiration and is linearly dependent on $V_{c,max}$. The introduced N limitation of $V_{c,max}$ in Section 2.2.3 also influences the N effect on maintenance respiration. N_l , N_s and N_r are the N contents of leaf, stem, and root, respectively, and the factor of 0.012 is from the unit conversion. Eq. (9) assumes the respiration rates in root and stem have the same dependence on N content as leaf. However, studies (Reich et al., 2008) have shown that the respiration rates at any common N concentration were consistently lower in leaves than in stems or roots on average. Thus, we introduce two PFT-specific parameters ($ResA_S$, $ResA_R$) from field observations (Wang et al., 2006; Yang et al., 1992) to adjust root and stem respirations. Their values are listed in Table 2.

$$R_{pm,Nlimit} = 0.012R_{dc} \frac{N_l + ResA_S * N_s + ResA_R * N_r}{N_l} \quad (10)$$

Table 2. The values of $ResA_S$ and $ResA_R$ for each plant function type (PFT).

PFT	Broadleaf deciduous	Broadleaf Evergreen	Needleleaf Evergreen	C3 grass	C4 grass	shrub	tundra shrub
$ResA_S$	1.36	1.36	1.44	1.0	1.0	1.25	1.25
$ResA_R$	1.72	1.72	1.95	1.3	1.3	1.40	1.40

290 Since $ResA_S$ and $ResA_R$ are generally larger than 1, new R_{pm} is larger than the original one, and the increased respiration due to the nitrogen limitation will decrease the NPP.

2.2.5 N limitation on LAI based on plant phenology

Studies (Aerts and Berendse, 1988; Thomas et al., 2015) show that leaf turnover and aboveground productivity are related to nutrient availability and that plant N processes can potentially give rise to lags on phenology. In TRIFFID, a leaf phenology parameter, p , (Cox, 2001) is introduced to represent the vegetation's phenological status, to calculate the leaf drop rate, and to adjust the model-simulated maximum possible LAI, which is based on carbon balance, ($LAI_{balance}$), to actual LAI and produce realistic phenology.



$$LAI = p \times LAI_{balance} \quad (11)$$

and

$$300 \quad \frac{dp}{dt} = \begin{cases} -\gamma_p & \gamma_{lm} > 2\gamma_0 \\ \gamma_p(1-p) & \gamma_{lm} \leq 2\gamma_0 \end{cases} \quad (12)$$

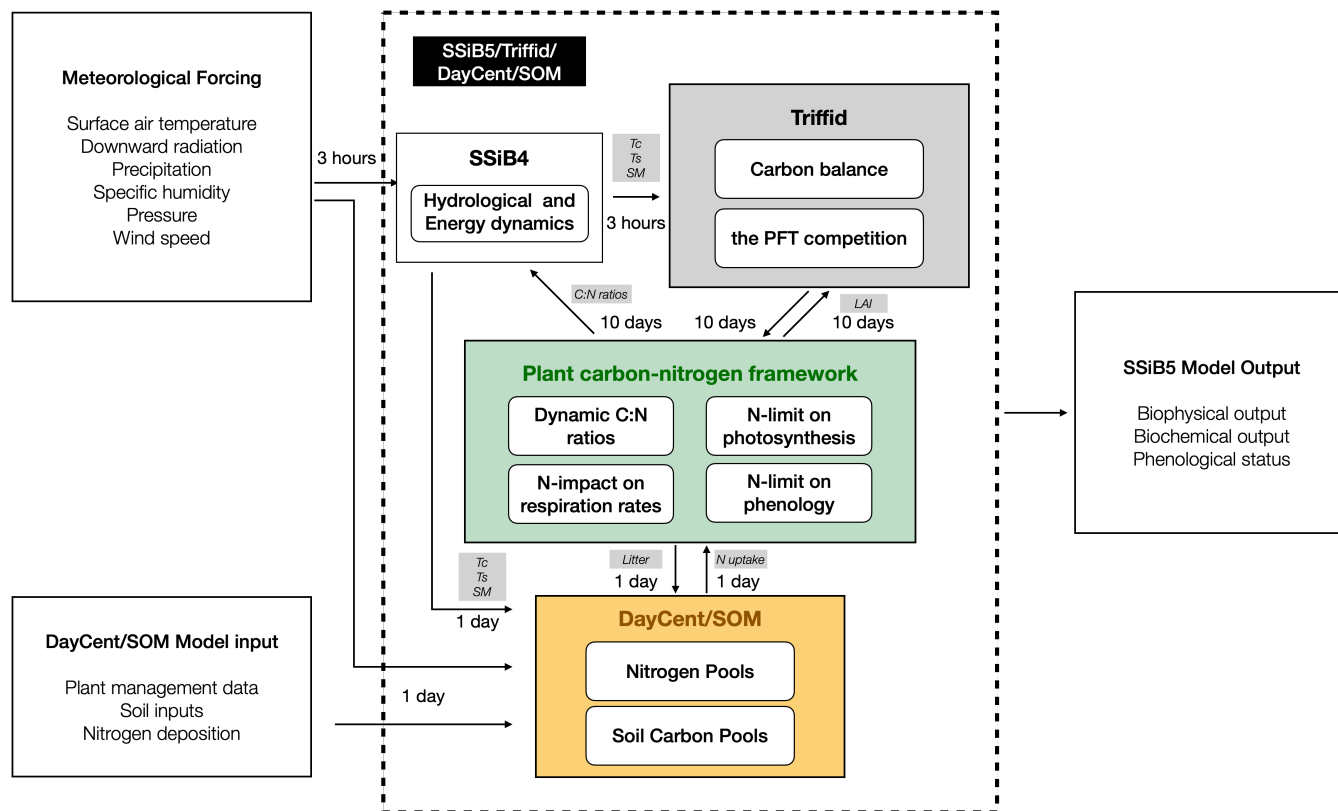
where leaf constant absolute drop rate $\gamma_p = 20 \text{ yr}^{-1}$, the leaf mortality rate γ_{lm} is a function of temperature T (Cox, 2001), and the minimum leaf turnover rate $\gamma_0 = 0.25$ (Cox, 2001). This phenology parameter, p , indicates that “full leaf” is approached asymptotically during the growing season, and p is reduced at a constant absolute rate when the mortality rate is larger than a threshold value. Otherwise, p increases but the rate of increase is reduced as the growing season evolves. To
305 reflect the N limitation in SSiB5/TRIFFID/DayCent-SOM, we assume p is limited by N availability with the new nitrogen limited $p_{N \text{ Limit}}$ determined by

$$p_{N \text{ Limit}} = f(N) \times p \quad (13)$$

where $f(N)$ is calculated in section 2.2.3.

2.2.6 The computational flow of SSiB5/TRIFFID/DayCent-SOM

310 In SSiB5/TRIFFID/DayCent-SOM, SSiB5 provides GPP, autotrophic respiration, and other physical variables such as canopy and soil temperatures and soil moisture every 3 hours for TRIFFID (Fig. 3). TRIFFID accumulates the GPP from SSiB5 and produces biotic C, PFT fractional coverage, vegetation height, and LAI every ten days, which are used to update surface properties in SSiB5, such as albedo, roughness length, and aerodynamic/canopy resistances. The plant C-N framework uses the meteorological forcings (i.e., air temperature, humidity, wind, radiation, and precipitation) and physical variables (i.e., soil
315 moisture and soil temperature) provided by SSiB5 every 3 hours and the biophysical properties (vegetation fraction and biotic C) provided by TRIFFID, which is updated every ten days. The plant C-N interface framework calculates dynamic C/N ratios, N-limited photosynthesis, and N-impacted respiration rate every 3 hours. The C loss and potential N uptake are accumulated within one day in the C-N Interface Framework and plant C and N litter fall are transferred to DayCent-SOM at the end of the day. DayCent-SOM calculates inorganic N available for plant N uptake (N_{avail}) and N losses from nitrate leaching and N-
320 trace gas emissions each day. TRIFFID updates the vegetation dynamics based on C balance on day 10, including PFT competition. The updated vegetation dynamics are transferred to SSiB5 to calculate N-limited phenology to reflect N impact on the C cycle, which is significant during the growth season.



325 **Figure 3.** Flowchart of plant carbon-nitrogen interactions in SSiB5/TRIFFID/DayCent-SOM; main variables are listed between two modules. Notes: Tc: canopy temperature; Ts: land surface temperature; SM: soil moisture; GPP: gross primary productivity; Res: autotrophic respiration.

2.3 Model forcing and validation data

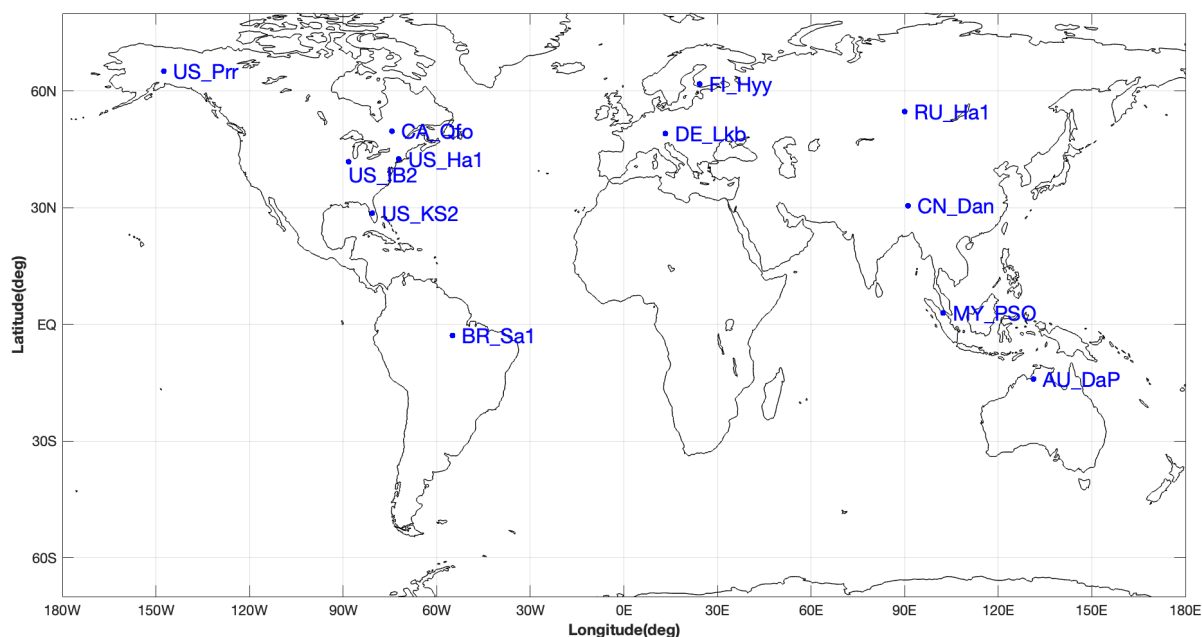
330 Long term measurements from flux tower sites with different PFTs and global satellite-derived products are employed as references to systematically assess the effects of this coupling framework and N limitation on the terrestrial carbon cycle. Flux tower sites data are presented in section 2.3.1. The global meteorological forcing and validation data are listed in sections 2.3.2 and 2.3.3 separately.

2.3.1 Ground measurement data

335 To validate the coupled model, twelve sites with representative biome types and climate zones were selected to evaluate the simulations of seasonal patterns of GPP, sensible heat flux, and latent heat flux. The driving data were a half-hourly dataset, including air temperature, specific humidity, wind velocity, air pressure, precipitation, and short- and long-wave radiation data



from the FLUXNET 2015 dataset (Pastorello et al., 2020). The geographical distribution of selected FLUXNET 2015 sites is displayed in Figure 4 and the detailed site information is listed in Table 3.



340

Figure 4. Geographical distribution of selected FLUXNET 2015 sites. The information of these FLUXNET sites is listed in Table 1.

Table 3. FLUXNET sites, latitude (LAT), longitude (LONG), plant function type (PFT), and time frame (Time) used for SSiB5/TRIFFID/DayCent-SOM model validation.

Site_ID	Site name	LAT	LONG	PFT	Time
AU_DaP	Daly River Savanna	-14.06	131.32	C4 grass	2007-2013
BR-Sa1	Santarem-Km67-Primary Forest	-2.86	-54.96	Broadleaf Evergreen	2002-2011
CA_Qfo	Quebec - Eastern Boreal, Mature Black Spruce	49.69	-74.34	Needleleaf Evergreen	2003-2010
CN-Dan	Dangxiong	30.50	91.07	C3 grass	2004-2005
DE_Lkb	Lackenberg	49.10	13.30	Needleleaf Evergreen	2009-2013
FI_Hyy	Hyytiala	61.85	24.29	Needleleaf Evergreen	1996-2014
MY_PSO	Pasoh Forest Reserve	2.97	102.31	Broadleaf Evergreen	2003-2009
RU_Ha1	Hakasia steppe	54.73	90.00	C3 grass	2002-2004
US_Ha1	Harvard Forest EMS Tower (HFR1)	42.54	-72.17	Broadleaf deciduous	1991-2012
US_IB2	Fermi National Accelerator Laboratory- Batavia (Prairie site)	41.84	-88.24	C3 grass	2004-2011
US-KS2	Kennedy Space Center (scrub oak)	28.61	-80.67	Shrub	2003-2006
US_Prr	Poker Flat Research Range Black Spruce Forest	65.12	-147.49	Needleleaf Evergreen	2010-2014



345 **2.3.2 Meteorological forcing data**

The Princeton global meteorological dataset for land surface modelling (Sheffield et al., 2006) was used to drive SSiB4/TRIFFID global simulations from 1948 to 2007 at 1° x 1° spatial resolution and a 3-hour temporal interval. This dataset, including surface air temperature, pressure, specific humidity, wind speed, downward short-wave radiation flux, downward long-wave radiation flux, and precipitation, was constructed by combining a suite of global observation-based datasets with
350 the National Center for Environmental Prediction/National Center for Atmospheric Research reanalysis data.

2.3.3 Global remote-sensing data

To assess the climatological status, variation, and trends of simulated LAI, two widely used global LAI products were used as references in this study: the Global Inventory Modeling and Mapping Studies (GIMMS) LAI and the Global LAnd Surface Satellite (GLASS) LAI. GIMMS-LAI is based on the third generation of Normalized Difference Vegetation Index (NDVI3g) from the GIMMS group and an Artificial Neural Network model (Zhu et al., 2013). GIMMS-LAI provides a 1/12-degree
355 resolution, 15-day composites, and spans July 1981 to December 2011. GLASS-LAI is generated from Advanced Very High Resolution Radiometer (AVHRR) (from 1982 to 1999 with 0.05-degree resolution) and Moderate Resolution Imaging Spectroradiometer (MODIS, from 2000 to 2012 with 1 km resolution) reflectance data using general regression neural networks (Xiao et al., 2014). GIMMS and GLASS LAI and the meteorological forcing data for the overlap period of 1982 to
360 2007 were remapped to 1-degree spatial resolution and a monthly temporal interval.

The Model Tree Ensemble (MTE) GPP product (Jung et al., 2009) was used as a reference to evaluate simulated GPP. MTE is based on a machine learning technique in which the model is trained to predict the five C fluxes at FLUXNET sites driven by observed meteorological data, land cover data, and the remotely-sensed fraction of absorbed photosynthetic active radiation (Jung et al., 2009). The trained model was then applied at the grid scale driven by gridded forcing data. MTE-GPP data were
365 resampled to 1-degree spatial and a monthly temporal resolution. However, the MTE data do not include CO₂ fertilization. Liu et al. (2019) discuss this issue and indicate that the lack of CO₂ fertilization mainly affects the trend. Since this paper focuses on climatological mean as well as differences between different experiments in which the CO₂ fertilization effect would be largely cancelled, the missing CO₂ fertilization in the FLUXNET-MTE is not a factor in interpreting our results.

3 Experimental design

370 To illustrate the reliability of the schemes which represent different processes of plant N in our framework, we first evaluated the model's short-term performance using in-situ measurements (section 3.2). Then, four sets of sensitivity experiments were designed to quantify the major effects of the plant N process and the relative contributions of different plant N processes on the terrestrial ecosystem carbon cycle (section 3.3).



3.1 Initial condition for the dynamic vegetation model

375 The initial condition of the dynamic vegetation SSiB4/TRIFFID needs to be obtained from a long-term equilibrium simulation (Zhang et al., 2015). There are different ways to initialize the surface condition for the quasi-equilibrium simulation. Following previous SSiB4/TRIFFID studies (Huang et al., 2020; Liu et al., 2019; Zhang et al., 2015), we set up the initial condition for the run using the SSiB vegetation map and SSiB vegetation table, which are based on ground surveys and satellite-derived information (Dorman and Sellers, 1989; Sellers et al., 1986; Xue et al., 2004; Zhang et al., 2015) with 100% occupation at each grid point for the dominant PFT and zero for other PFTs. We then ran the SSiB4/TRIFFID model with the climate forcing and the atmospheric CO₂ concentration at 1948 level for 100 years to reach equilibrium conditions. The vegetation and soil conditions from the equilibrium results were used as the initial conditions for the subsequent model runs.

Determining the initial conditions for SSiB5/TRIFFID/DayCent-SOM was carried out as described for SSiB4/TRIFFID with one additional step in order to initialize global soil C and N levels. We saved 60 years of daily litter C/N inputs and soil temperature and moisture conditions from SSiB4/TRIFFID that were based on historical meteorological forcings (1948-2007). An offline version of DayCent-SOM was run for 2000 years for each grid cell using these 60 years of data, repeated over and over, to determine quasi-equilibrium soil C & N levels; these soil C and N values were read in by SSiB5/TRIFFID/DayCent-SOM at the start of the global simulation in 1948.

3.2 Site-level validation

390 This paper focuses on the impact of N processes on the climatology of the global carbon cycle. Most current Dynamic Global Vegetation Models (DGVMs) are mainly focused on long-term (decadal to thousands of years or even longer) simulations at global scale; the diurnal and seasonal variations are not a subject for their modelling. Moreover, adequate long-term in-situ measurements are also not available for comparison. However, since the SSiB5/TRIFFID is a process-based model, we can evaluate the model's short-term performance using in-situ measurements.

395 Twelve sites with representative biome types and climates zones (Table 3 and Fig. 4) were selected to evaluate the simulations of seasonal patterns of fluxes over these sites. The site-level simulations were conducted by SSiB4/TRIFFID (a C-only model) and SSiB5/TRIFFID/DayCent-SOM separately to validate the model's performance. The model results were compared against observed daily data obtained by the flux tower including GPP, sensible heat flux, and latent heat flux.

3.3 Global 2-D offline control run and sensitivity runs

400 In this study, the SSiB4/TRIFFID and the SSiB5/TRIFFID/DayCent-SOM were applied to conduct a series of global 2-D offline runs (Table 4). All these runs employed the quasi-equilibrium simulation results as the initial condition, then were driven by the historical meteorological forcing from 1948 through 2007. The run using the SSiB4/TRIFFID is referred to as the control run (Exp. SSiB4 hereafter). Using the control simulation, we first evaluated the ability of the model to produce the climatology and variability of several biotic variables by comparing the results to multiple observation-based datasets. In



405 addition to the control run, six sets of sensitivity experiments were conducted to quantify the major effects of the N process and C-N interface coupling methodology on the C cycle. These sensitivity experiments were designed as follows:

(1) Nitrogen limitation on photosynthesis (Exp. NIPSN): The same meteorological forcing used for the control (Exp. SSiB4) drives the model, but dynamic C/N ratios and N limitation on $V_{c,max}$ (Eq. 6) are introduced. The difference between Exp. SSiB4 and Exp. NIPSN indicates the effect of N limitation on photosynthesis.

410 (2) Nitrogen impact on Respiration rate (Exp. NIResp): The model was driven by the same meteorological forcing used for Exp. SSiB4, but dynamic C/N ratio and N impacts on autotrophic respiration (Eq. 10) are introduced. The difference between Exp. SSiB4 and Exp. NIResp indicates the effect of N impact on respiration rate.

(3) Nitrogen limitation on Phenology (Exp. NIPhen): The model was driven by the same meteorological forcing used for Exp. SSiB4, but dynamic C/N ratio and N impacts on phenology (Eq. 13) are introduced. The difference between Exp. SSiB4 and
 415 Exp. NIPhen indicates the effect of nitrogen limitation on phenology.

(4) SSiB5/TRIFFID/DayCent-SOM (Exp. SSiB5): The model was driven by the same meteorological forcing used for Exp. SSiB4, but all four C-N coupling processes in the framework, i.e., dynamic C/N ratio, N impacts on photosynthesis, autotrophic respiration, and phenology, are introduced. The difference between Exp. SSiB4 and Exp. SSiB5 indicates the effect of N dynamics, especially the sensitivity of C cycle variability and trend to N process coupling. Furthermore, the difference between
 420 Exp. NIPSN and Exp. SSiB5 indicates the uncertainty (or possible errors) due to missing N effect on autotrophic respiration and phenology in the coupling framework.

Although the model runs were from 1948 to 2007, we only present the results from 1982-2007 to avoid spinning up for the SSiB5/TRIFFID/DayCent-SOM after SSiB4/TRIFFID and DayCent-SOM each reached their historical equilibrium conditions. Since the results from Exps. SSiB5 and NIPSN showed statistically significant differences from Exp. SSiB4 over many parts
 425 of the world, in the following discussion we will mainly focus on these two experiments' differences with Exp. SSiB4.

Table 4. Experimental design

100-year equilibrium	<i>Initial condition</i> →	Real-forcing simulation 1948-2007
<i>Fixed climatology forcing</i>		<i>Transient forcing</i>
Control experiment		SSiB4: Control experiment NIPSN: Nitrogen limitation on photosynthesis(V_{max}), Eq.6 NIResp: Nitrogen impact on Respiration rate, Eq.10 NIPhen: Nitrogen limitation on Phenology, Eq. 13 SSiB5: including all four nitrogen processes



4. Results

To test this framework, measurements from flux tower sites with different PFTs and global satellite-derived products from 1982-2007 are employed as references. The results from site simulation and global 2-D simulations are presented in sections 4.1 and 4.2., respectively. As mentioned in section 2, the framework takes some plant N metabolism processes into account. To illustrate the relative contributions of different plant N processes on the terrestrial ecosystem carbon cycle, four sets of sensitivity experiments were designed (Table 4). The analyses are presented in section 4.2.

4.1 Evaluations using the measurements from flux tower sites

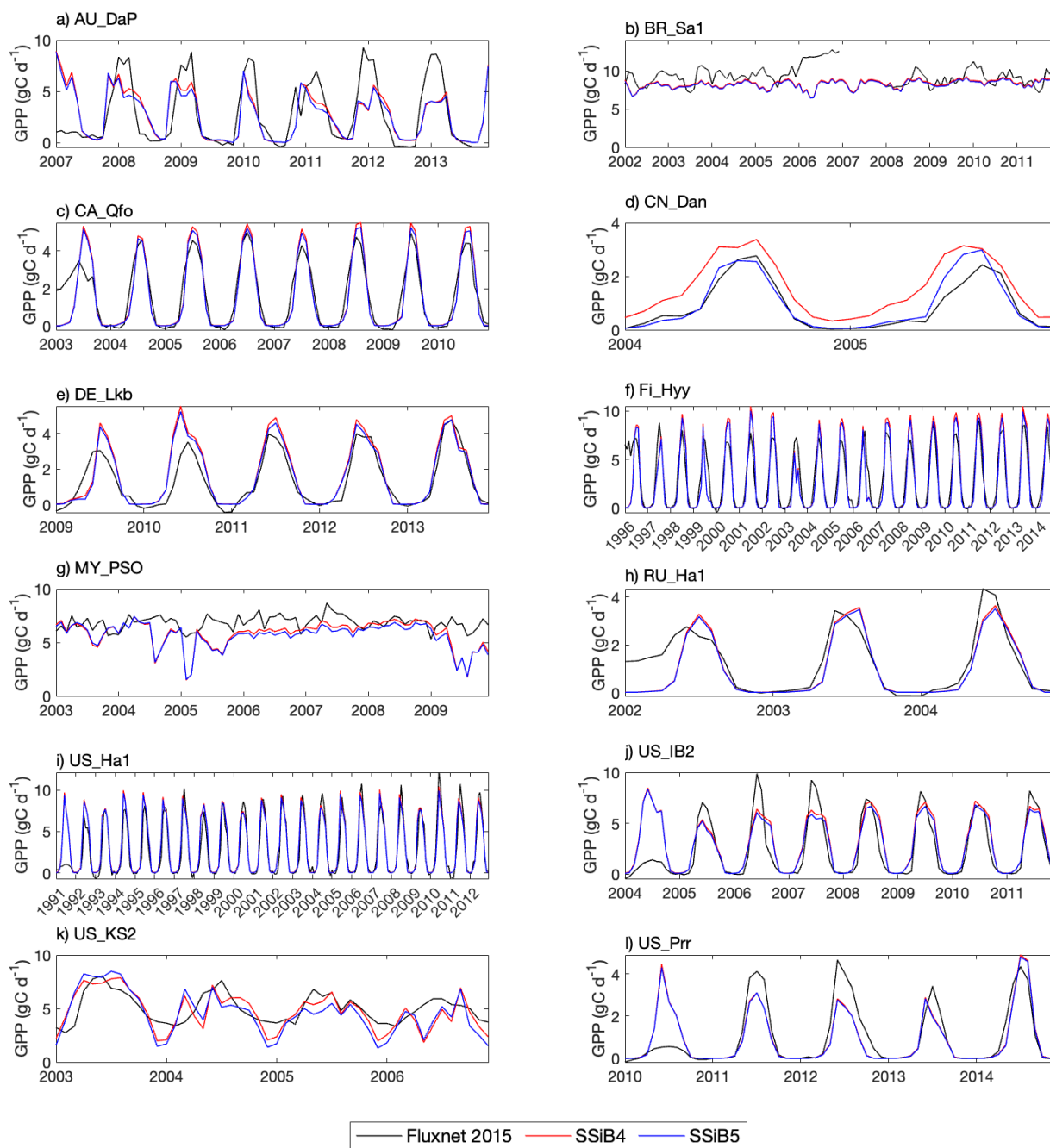
Land models with dynamic vegetation and nitrogen processes normally focus on the long-term climate simulation with large spatial scales. In this section, we validate the model performance for twelve sites with several years of simulation (Table 3) to ensure that as a process-based model, the SSiB5/TRIFFID in the short term simulation is still able to properly represent the surface processes at seasonal scales after introducing the DayCent-SOM through the interface coupling framework. This evaluation also provides a glance at the model's performance at several sites with various climate and PFTs (Table 3) with short-term data to gain preliminary confidence for further evaluation.

Figures 5, 6, and 7 show that both SSiB4 and SSiB5/TRIFFID/DayCent-SOM produce a reasonable seasonal cycle for GPP, sensible heat, and latent heat fluxes, respectively, and that the results are close to observation. Table 5 summarizes the major results. We use bias, root-mean-squared error (RMSE), as well as standard deviation to assess model performance against the in-situ site measurements. When we evaluate the 12 sites average, the biases for GPP and sensible and latent heat fluxes are decreased by about 7%, 18%, and 2 %, respectively. The average RMSEs over the 12 sites for these three variables are also decreased by about 2%, consistent with the reduction in bias. Furthermore, the SSiB5/TRIFFID/DayCent-SOM produces closer standard deviation for GPP, sensible heat flux, and latent heat flux than SSiB4/TRIFFID for the 12-site averages. By and large, in these short-term simulations with specified initial vegetation conditions, both SSiB4 and SSiB5 produce reasonable GPP and surface heat fluxes compared with in-situ measurements, but adding N processes (SSiB5) shows a slight improvement for the 12-site average. Although these improvements are rather marginal (except the bias reduction for sensible heat), the results nevertheless demonstrate that, with short-term simulation, model simulations' improvement is rather consistent.

With closer checking of the SSiB4 to SSiB5 results at each site, the results display various characteristics. For instance, some sites mainly show the improvement in both bias and RMSE, while others show improvement only in one or the other. Moreover, while some sites show improvement in all three variables (GPP, latent and sensible heat fluxes), others only show improvement for one or two variables. It should be pointed out that SSiB4 and SSiB5 are mainly used for global studies. For validation of in-situ measurements, proper optimization of some site-specific soil and vegetation parameters is necessary (Xue et al., 1996, 1997). In this study, no model parameters were optimized during this validation exercise for a better fit between simulated results and FLUXNET measurements. The discussions above lead us to conduct long-term experiments at a global scale to



460 comprehensively investigate the N process effect and to help understand mechanisms governing the global carbon cycle, which will be discussed in the following section.



465 **Figure 5.** Simulated seasonal variations of GPP against observations at twelve FLUXNET sites representing different SSiB5 PFTs.
 Note: the information about these FLUXNET sites is listed in Table 3.

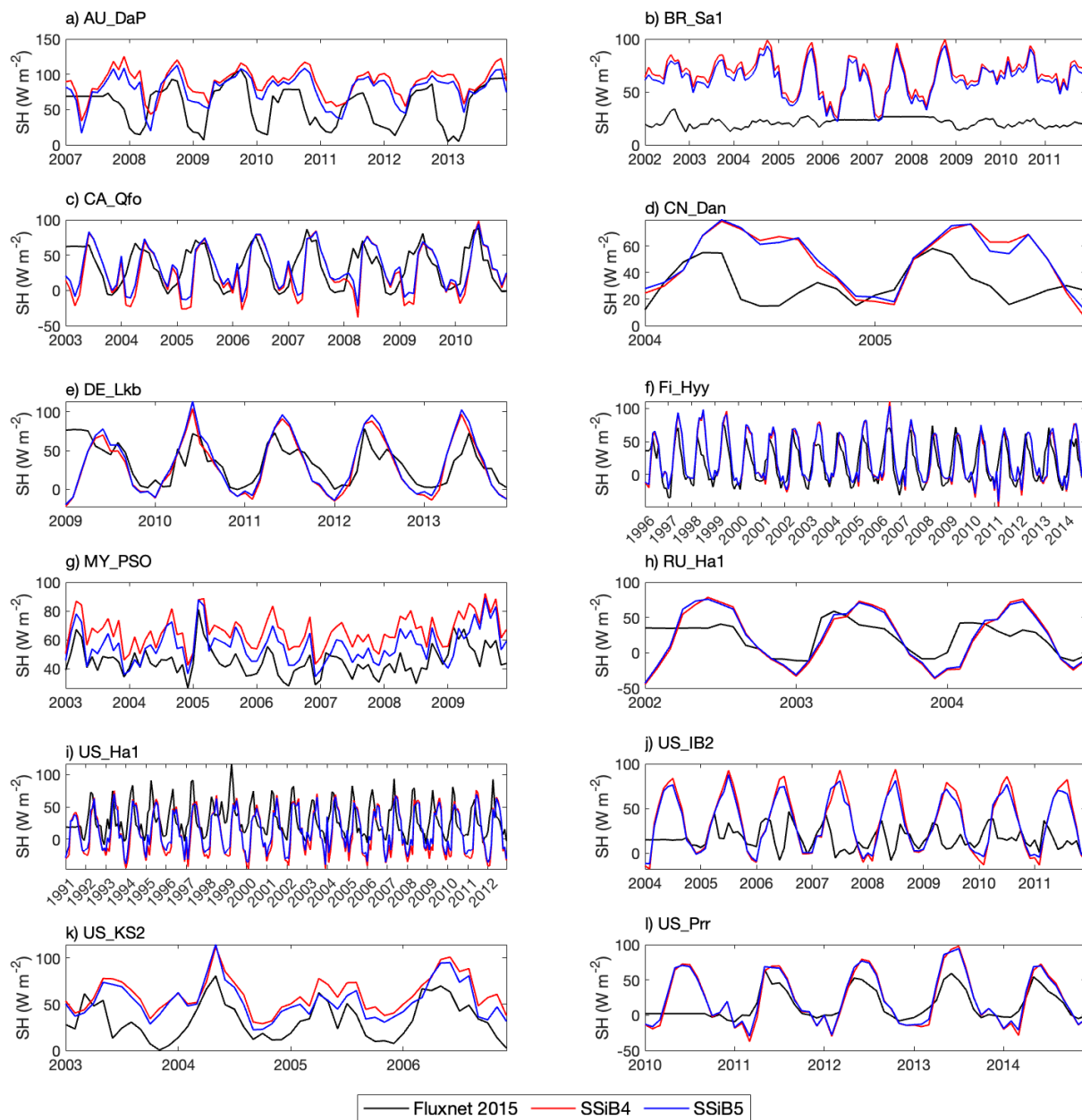
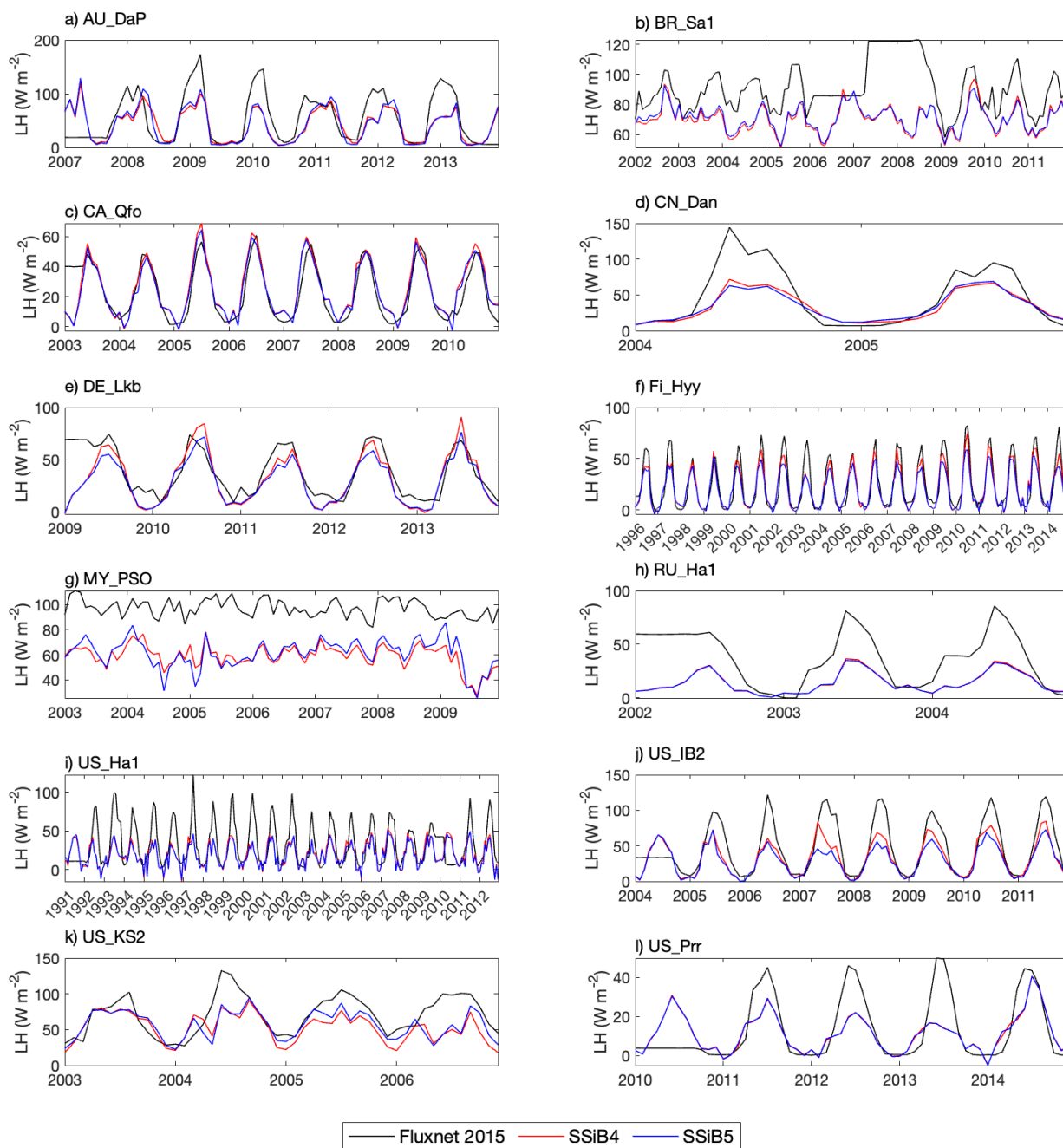


Figure 6. Same as Figure 5, but for sensible heat flux.



470

Figure 7. Same as Figure 5, but for latent heat flux.



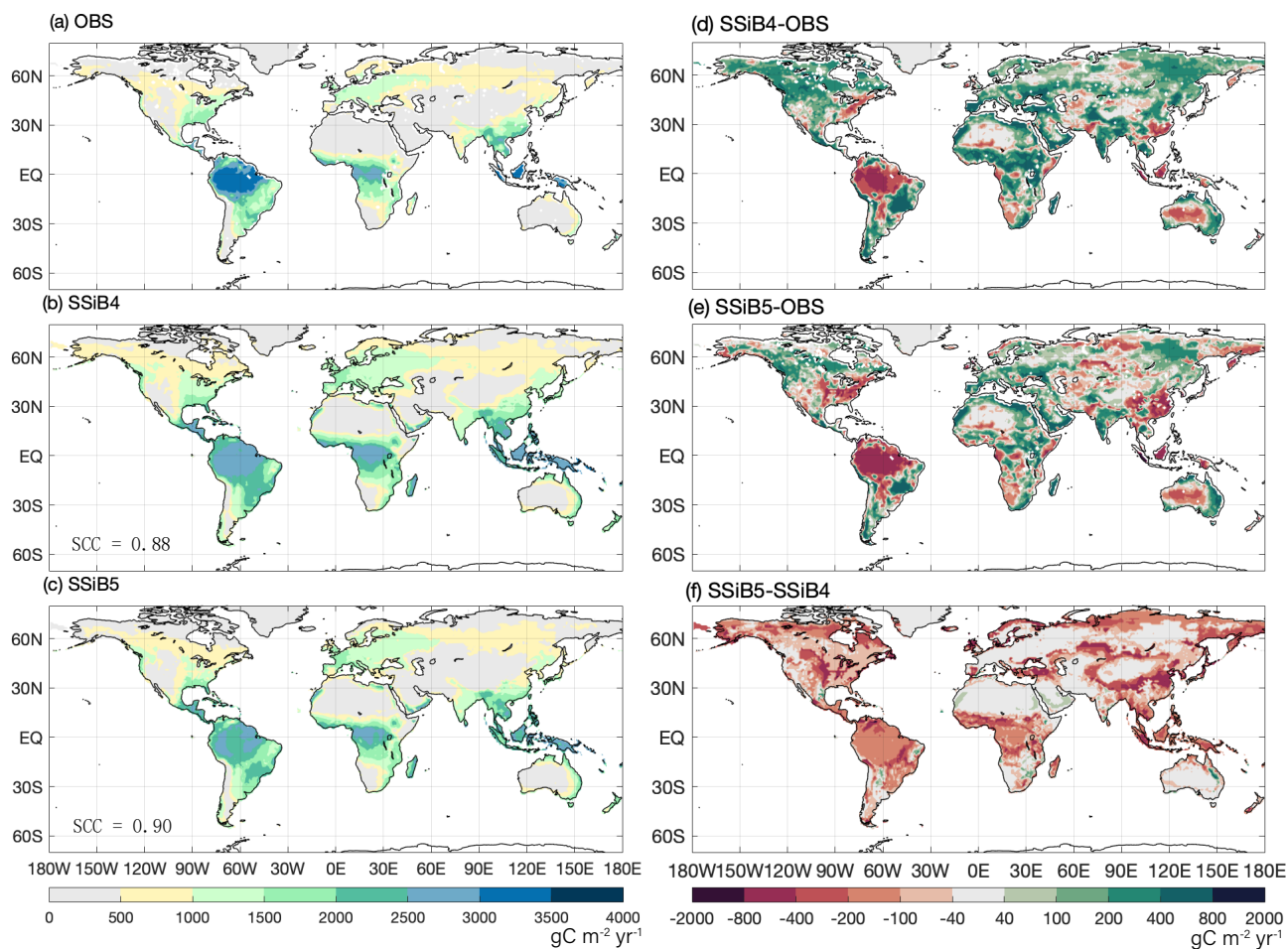
Table 5. The GPP, sensible heat flux, and latent heat flux intercomparisons of bias, standard deviation and RMSE between SSiB4 and SSiB5 over twelve sites.

	Site_ID	Bias		Standard deviation			RMSE	
		SSiB4	SSiB5	Fluxnet	SSiB4	SSiB5	SSiB4	SSiB5
GPP (g C d ⁻¹)	AU_DaP	0.05	-0.05	3.11	2.46	2.33	2.60	2.61
	BR-Sa1	-1.07	-1.20	1.31	0.57	0.55	1.77	1.84
	CA_Qfo	-0.05	-0.11	1.71	1.99	1.92	0.78	0.75
	CN-Dan	0.70	0.08	0.92	1.08	1.03	0.80	0.33
	DE_Lkb	0.34	0.25	1.50	1.80	1.71	0.80	0.74
	FI_Hyy	-0.11	-0.22	2.93	3.47	3.32	1.51	1.44
	MY_PSO	-1.02	-1.20	0.65	1.28	1.21	1.63	1.72
	RU_Ha1	-0.24	-0.27	1.29	1.31	1.27	0.69	0.69
	US_Ha1	0.36	0.27	3.31	3.36	3.30	1.31	1.28
	US_IB2	0.56	0.42	2.91	2.70	2.57	1.80	1.79
	US-KS2	-0.28	-0.52	1.37	1.76	2.01	1.35	1.54
	US_Prr	-0.08	-0.10	1.43	1.30	1.28	0.86	0.86
12-site average		0.41	0.38	1.87	1.92	1.88	1.33	1.30
Sensible Heat Flux (W m ⁻²)	AU_DaP	32.47	23.13	28.26	19.64	21.05	36.24	36.32
	BR-Sa1	45.29	40.94	4.04	16.32	15.98	25.61	25.07
	CA_Qfo	-7.04	-2.34	27.77	33.18	29.37	9.54	9.20
	CN-Dan	17.96	18.53	14.44	22.38	20.75	25.60	26.99
	DE_Lkb	-3.12	0.16	25.13	35.39	36.91	17.83	18.15
	FI_Hyy	5.53	7.20	28.17	33.57	33.63	8.99	10.91
	MY_PSO	20.49	10.86	10.03	11.30	11.98	39.22	37.99
	RU_Ha1	-0.14	0.84	21.71	39.19	38.02	29.42	29.67
	US_Ha1	-18.34	-15.80	24.40	33.71	29.42	24.33	24.66
	US_IB2	20.21	18.26	11.95	32.89	29.19	23.16	28.72
	US-KS2	27.74	20.81	21.01	19.17	20.14	27.31	24.73
	US_Prr	8.10	9.35	20.93	36.84	35.45	12.02	12.01
12-site average		17.20	14.02	19.82	27.80	26.82	23.27	22.70
Latent Heat Flux (W m ⁻²)	AU_DaP	-11.02	-10.83	45.72	30.03	33.93	36.24	36.32
	BR-Sa1	-20.47	-19.82	16.15	9.44	8.47	25.61	25.07
	CA_Qfo	2.21	0.96	18.06	18.63	17.56	9.54	9.20
	CN-Dan	-12.63	-12.57	42.39	22.13	20.77	25.60	26.99
	DE_Lkb	-7.39	-10.00	22.81	24.57	20.79	17.83	18.15
	FI_Hyy	-3.06	-4.84	23.22	19.21	16.64	8.99	10.91
	MY_PSO	-38.18	-36.18	7.07	9.24	11.64	39.22	37.99
	RU_Ha1	-22.89	-23.10	25.68	10.43	10.08	29.42	29.67
	US_Ha1	-11.94	-13.14	27.06	15.53	14.71	24.33	24.66
	US_IB2	-12.90	-17.38	36.91	24.68	20.70	23.16	28.72
	US-KS2	-17.74	-13.41	27.63	20.28	19.65	27.31	24.73
	US_Prr	-1.90	-1.87	16.44	9.62	9.68	12.02	12.01
12-site average		13.93	13.67	25.76	17.82	17.95	24.27	23.70



4.2 Evaluation of GPP and LAI at global scale

475 Since the SSiB model is mainly used for global study, in this section, we evaluate the model's performance using the observed
global GPP and LAI data. The simulated GPP averaged over 1982-2007 is compared to FLUXNET-MTE GPP (Jung et al.,
2011) to examine the impact of N processes and its coupling with C and ecosystem processes. Both SSiB4/TRIFFID (Exp.
SSiB4) and SSiB5/TRIFFID/DayCent-SOM (Exp. SSiB5) capture the distribution of global GPP (Fig. 8) and its latitudinal
distribution (Fig. 9a). The highest GPP occurs in the tropical evergreen forest and generally decreases with the increase in
480 latitudes in both the observations and the model simulation (Figs. 8 and 9a). Exp. SSiB4-simulated GPP has positive bias over
many parts of the world (Fig. 8d), including tropical Africa and the North American and eastern Siberian boreal regions, but
negative bias in some regions, mainly in the Amazon tropical forest. The simulated global GPP is $1082.36 \text{ g C m}^{-2} \text{ yr}^{-1}$ (Table
6), higher than the estimate, $862.86 \text{ g C m}^{-2} \text{ yr}^{-1}$ in FLUXNET-MTE (Jung et al., 2011). After introducing the N limitation for
three processes, the SSiB5 reduced the positive bias in SSiB4 over many parts of the world (Figs. 8e, 8f, and 9a). Exp. SSiB5's
485 global GPP prediction, $941.81 \text{ g C m}^{-2} \text{ yr}^{-1}$, is closer to observations compared to Exp. SSiB4, with a 16.3% reduction in the
bias (Table 6). Furthermore, the temporal correlation coefficients between observed and simulated monthly/annual mean GPPs
are increased from 0.46/0.98 (Exp. SSiB4) to 0.50/0.99 (Exp. SSiB5), respectively (Fig. 10), showing improvement in
simulation of the seasonal cycle in SSiB5. The correlation for interannual variability in SSiB4 is already very high (0.98).
SSiB5 shows no substantial improvement.



490

Figure 8. The 1982-2007 average gross primary production comparison for (a) FLUXNET-MTE GPP (OBS), (b) SSiB4/TRIFFID (SSiB4), and (c) SSiB5/TRIFFID/DayCent/SOM (SSiB5), and difference between (d) SSiB4-OBS, and (e) SSiB5-OBS, (f) SSiB5-SSiB4. Note: SCC indicates the spatial correlation coefficient between model simulation and satellite-derived datasets (OBS).

495

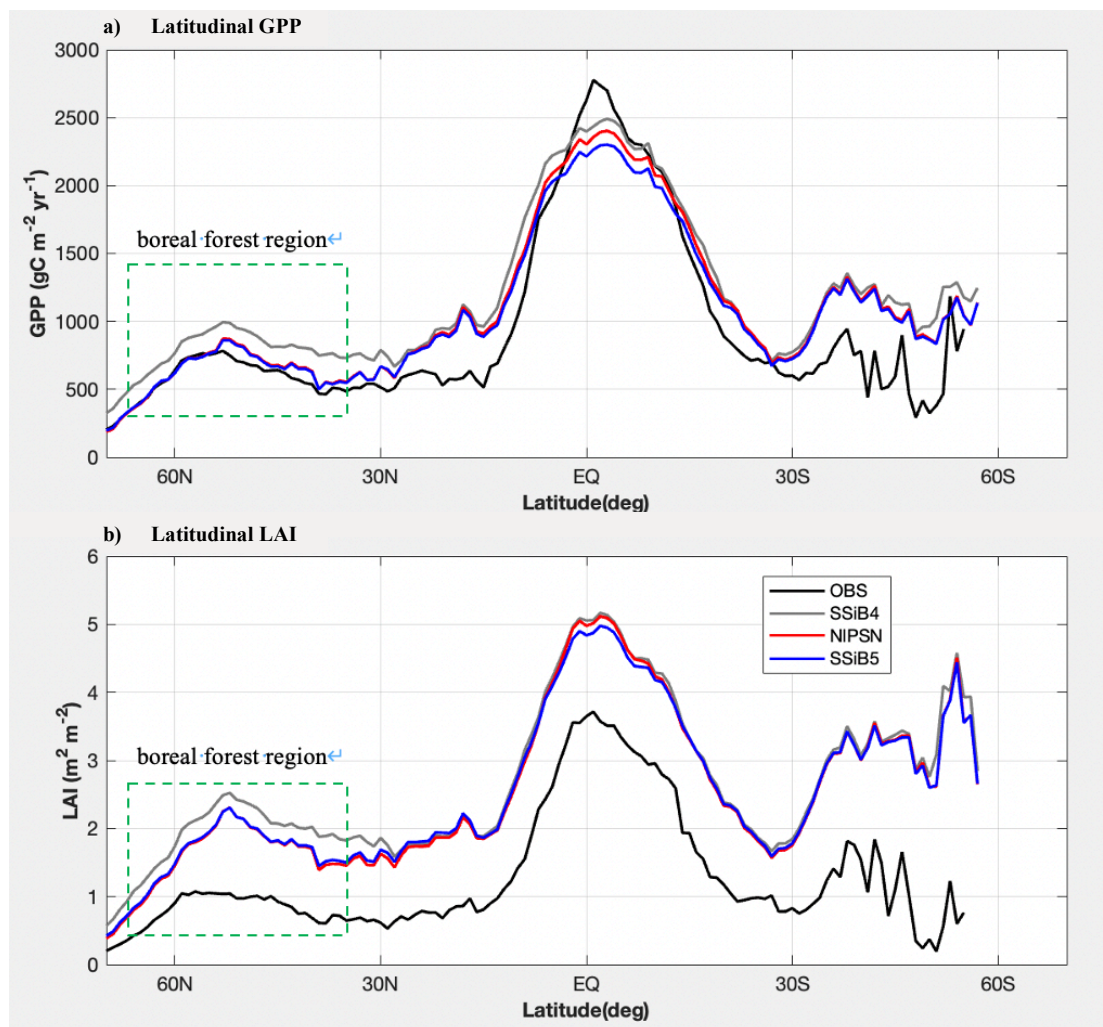


Figure 9. Intercomparisons of latitudinal LAI and GPP among OBS, SSiB4 (control), NIPSN (N limitation on photosynthesis only), and SSiB5 (all N processes) over the period 1982-2007.

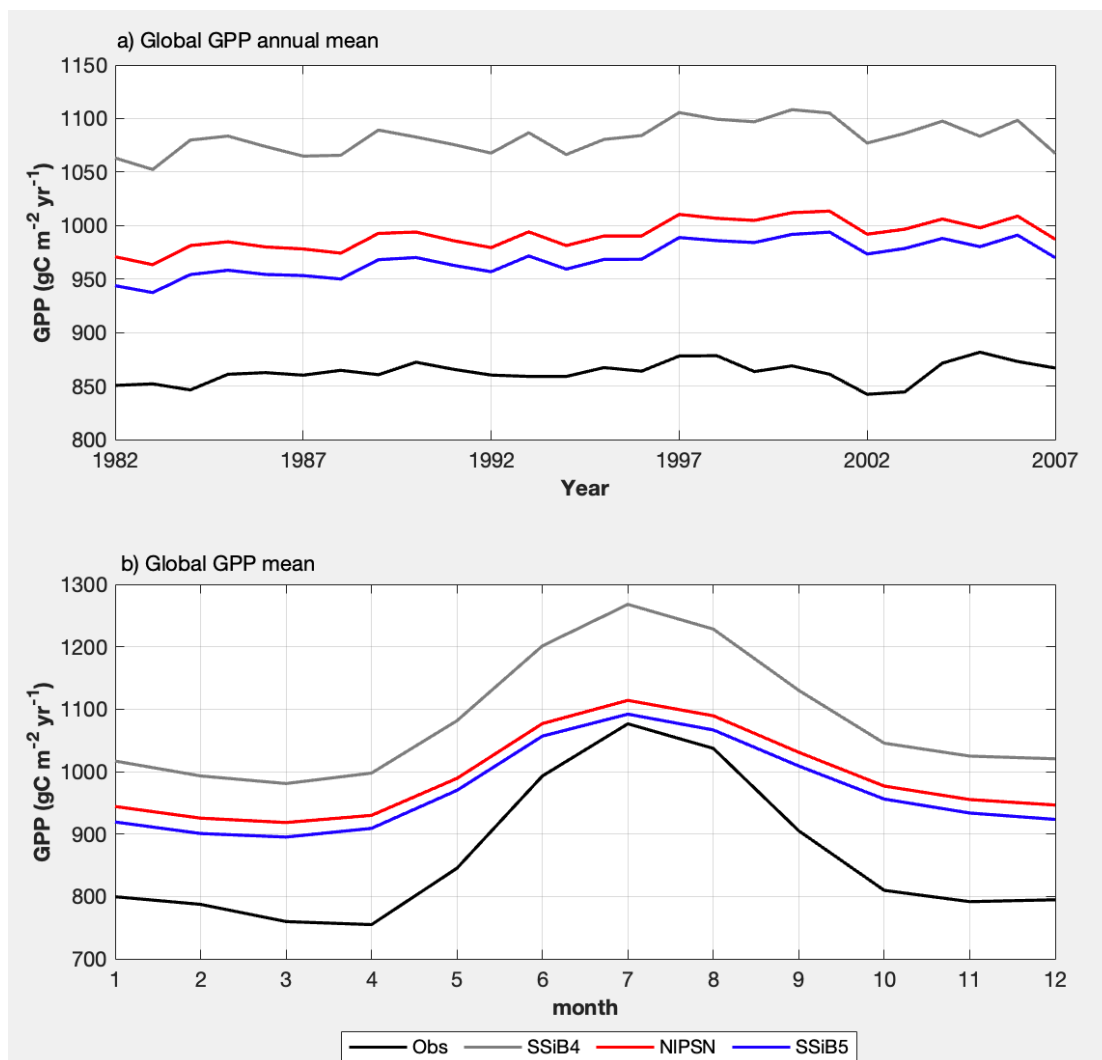


Table 6. Regional and Global GPP for (a) FLUXNET-MTE GPP (observation), (b) SSiB4 (control), (c) NIPSN (N limitation on photosynthesis only) and (d) SSiB5 (N limitation on photosynthesis, autotrophic respiration, and phenology).

Regions	Sub-regions	GPP Mean ($\text{gC m}^{-2} \text{yr}^{-1}$)							
		MTE		SSiB4		NIPSN		SSiB5	
		mean	bias	mean	bias	mean	bias	mean	bias
Arid and Semi-Arid Areas	West Africa	893		1147	254(28.5%)	963	70(7.9%)	915	22(2.5%)
	West NA	438		549	111(25.4%)	454	16(3.5%)	431	-7(-1.6%)
	SA Savanna	1665		1860	195(11.7%)	1763	98(5.9%)	1675	10(0.6%)
	East Africa	1228		1533	306(24.9%)	1427	199(16.2%)	1356	128(10.4%)
	East Asian semi-arid	1440		1470	30(2.1%)	1199	-241(-16.7%)	1139	-301(-20.9%)
NH High-Mid Latitude Areas	NA High-Mid Latitude	552		814	262(47.6%)	700	149(27.0%)	665	114(20.6%)
	Eurasian High-Mid	844		966	122(14.5%)	871	27(3.2%)	827	16(-2.0%)
Equator	Amazon Basin	2993		2668	-326(-10.9%)	2631	-362(-12.1%)	2500	-494(-16.5%)
	Southeast Asia	2778		2540	-238(-8.6%)	2419	-359(-12.9%)	2298	-480(-17.3%)
	Equator Africa	2522		2645	123(4.9%)	2611	89(3.5%)	2481	-42(-1.7%)
Subarctic Areas and Tibet	NA Subarctic	234		364	130(55.7%)	240	6(2.4%)	228	-6(-2.7%)
	Eurasian Subarctic	331		484	153(46.2%)	328	-3(-1.0%)	311	-20(-6.0%)
	Tibet	409		561	153(37.3%)	298	-111(-27.2%)	283	126(-30.8%)
Global		863		1082	220(25.4%)	991	129(14.9%)	942	79(9.1%)

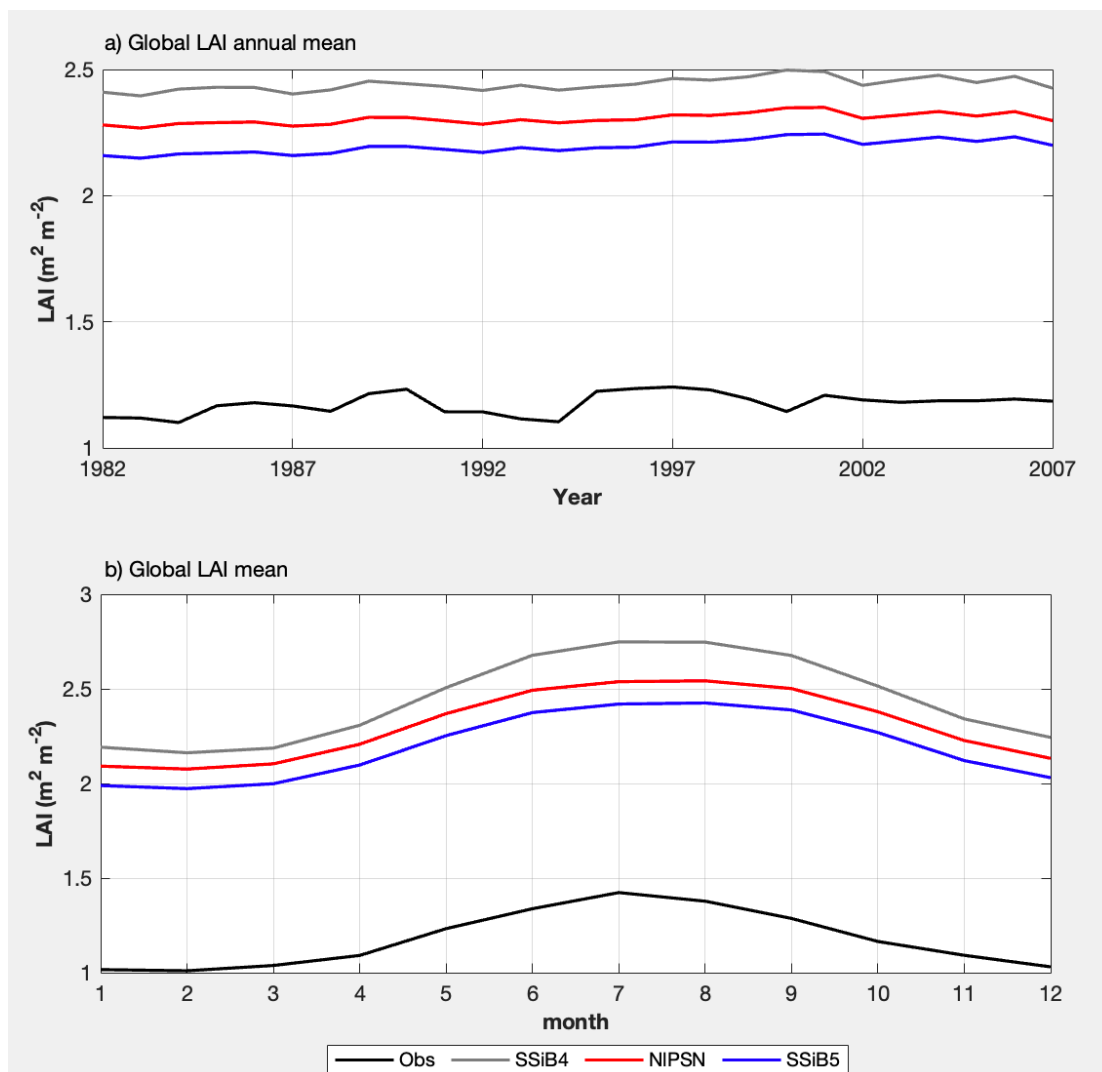
Note: the numbers in parentheses are relative biases: (bias/MTE mean)

505 The improvement, however, is not homogeneous over the globe but displays apparent regional characteristics. The GPP biases in tropical Africa, North American boreal region, South American savanna, and central U.S. show substantial reduction (Fig. 8f), which help improve the spatial distribution of SSiB5. The global spatial correlation coefficient increases from 0.88 to 0.90 (Fig. 8). Meanwhile, the GPP simulations in some regions, such as in the temperate East Asian mixed forest-grassland regions and in some areas in Siberia (Fig. 8), did not improve. In particular, the negative GPP bias in the Amazon is increased (Fig. 8f). This phenomenon has also appeared in the offline test in the Amazon site (the BR-Sal Site, Table 5). Du et al. (2020) indicate that phosphorus (P) has more effect in tropical areas. This paper mainly focuses on model development and preliminary global evaluation. More regional evaluation is necessary for further investigation, especially for the regions where the N limitation is not dominant.



515

Figure 10. Intercomparisons of global monthly/annual mean GPPs among OBS, SSiB4 (control), NIPSN (N limitation on photosynthesis only), and SSiB5 (all N processes) over the period 1982-2007.



520

Figure 11. Same as figure 10, but for LAI.

Furthermore, the N-limitation effect on the LAI simulation is also investigated. Both SSiB4 and SSiB5 produce reasonable spatial distribution compared with satellite-derived products (Figs. 12a-c). The highest LAI occurs in the tropical evergreen forest and decreases with latitude in both the observations and the model (Fig. 9b). Exp. SSiB5 also generally reduces the positive bias in simulated LAI compared to the control (Fig. 12f). The simulated LAI in Exp. SSiB4 has a global positive bias. After introducing three N limitation processes, the positive bias is reduced over most parts of the world (Fig. 12f). Globally, Exp. SSiB5 has an LAI bias of 0.94/1.12 for GIMMS/GLASS, respectively (Table 7), which is lower than the LAI bias of 1.26/1.44 for GIMMS/GLASS, respectively, in Exp. SSiB4, with a substantial 31.1% reduction in the bias (compared to GIMMS, Table 7). However, the positive bias still exists substantially over the globe (Fig. 12e). In a land model

525

530



intercomparison, the positive LAI prevailed in almost every dynamic vegetation model (Murray-Tortarolo et al., 2013). Our study shows that imposing N limitation is an adequate step to overcome the dynamic vegetation models' systematic LAI positive bias, but the issue is still not solved and requires more investigation. In addition, the correlation coefficients between observed and simulated monthly/annual average LAIs are improved from 0.49/0.97 (Exp. SSiB4) to 0.51/0.98 (Exp. SsiB5) (Fig. 11).

535 (Fig. 11).

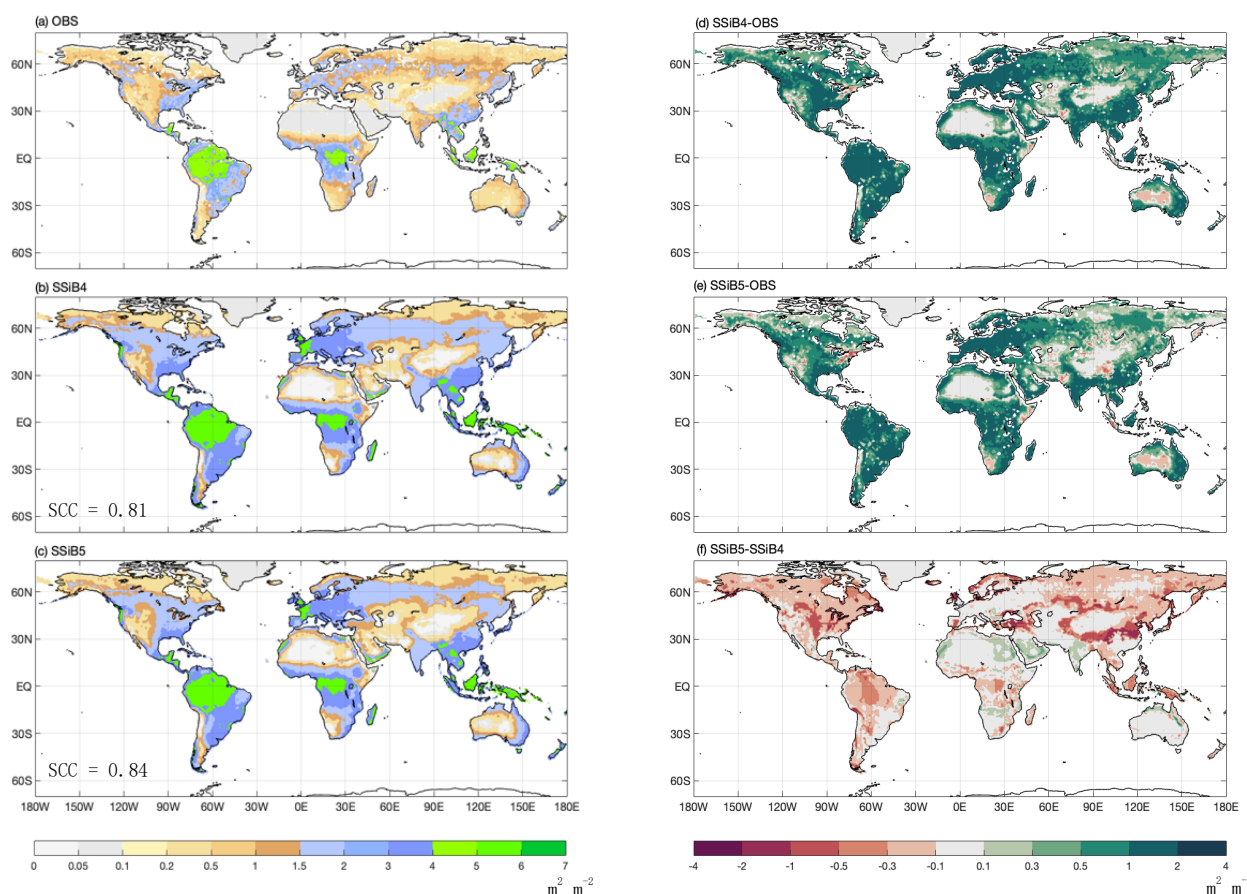


Figure 12. Same as Figure 8, but for LAI.

Note: SCC indicates the spatial correlation coefficient between model simulation and GIMMS LAI (OBS).

540

It is interesting to note that despite the global general LAI reduction, the SsiB5 slightly increased LAI estimation in North Africa and India (Fig. 12). The N impacts on phenology and respiration cause a slight shift in the vegetation from shrub (N. Africa) or C4 grass (India) to C3 grass in these areas, which contributes to the GPP and LAI increase (Fig. 13). Furthermore, in areas such as the Amazon, East Asian mixed forest-grassland regions, SsiB5 only improves the LAI simulation, not the

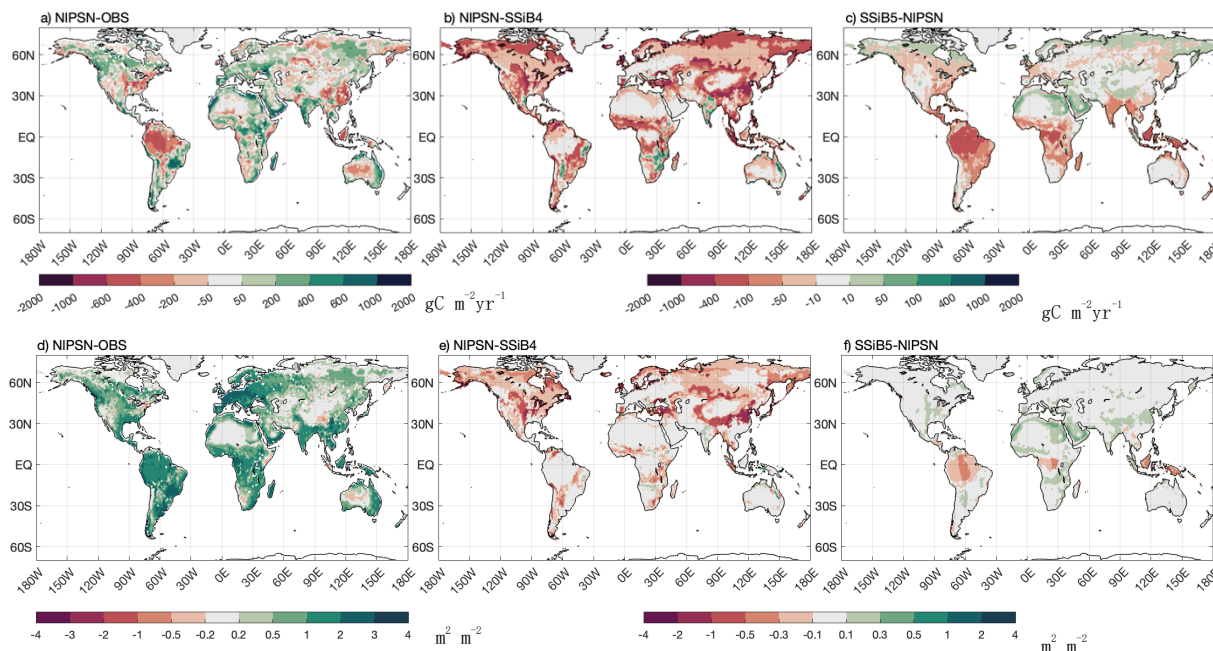


545 GPP simulation. We will further identify the effect of N limitation on the photosynthesis process and other processes on simulated GPP and LAI. More observational data are necessary to gain more understanding.

550 **Table 7.** Regional and Global LAI for (a) GIMMS LAI (observation), (b) GLASS LAI (second observation), (c) SSiB4 (control), (d) NIPSN (N limitation on photosynthesis only) and (e) SSiB5 (N limitation on photosynthesis, autotrophic respiration, and phenology). The bias is relative to GIMMS LAI.

Regions	Sub-regions	LAI Mean ($m^2 m^{-2}$)									
		GIMMS		GLASS		SSiB4		NIPSN		SSiB5	
		mean	bias	mean	bias	mean	bias	mean	bias	mean	bias
Arid and Semi-Arid Areas	West Africa	1.08	1.01	-0.07(-6.5%)	2.04	0.96(88.9%)	1.89	0.81(75.0%)	1.73	0.65(60.2%)	
	West NA	0.62	0.49	-0.13(-21.0%)	1.38	0.76(122.6%)	1.18	0.56(90.3%)	1.09	0.47(75.8%)	
	SA Savanna	1.99	1.91	-0.18(-4.0%)	3.34	1.35(67.8%)	3.23	1.24(62.3%)	2.97	0.98(49.2%)	
	East Africa	1.59	1.55	-0.04(-2.5%)	3.02	1.43(89.9%)	2.89	1.30(81.8%)	2.66	1.07(67.3%)	
	East Asian semi-arid	1.60	1.36	-0.24(-15.0%)	3.35	1.75(109.4%)	2.84	1.24(77.5%)	2.61	1.01(63.1%)	
NH High-Mid Latitude Areas	NA High-Mid Latitude	0.84	0.49	-0.35(-41.7%)	1.91	1.07(127.4%)	1.66	0.82(97.6%)	1.53	0.69(82.1%)	
	Eurasian High-Mid	1.14	0.57	-0.57(-50.0%)	2.29	1.15(100.9%)	2.08	0.94(82.5%)	1.91	0.77(67.5%)	
Equator	Amazon Basin	4.19	4.08	-0.11(-2.6%)	6.01	1.82(43.4%)	5.98	1.79(42.7%)	5.50	1.31(31.3%)	
	Southeast Asia	3.93	3.88	-0.05(-1.3%)	4.68	0.75(19.1%)	4.68	0.75(19.1%)	4.31	0.38(9.7%)	
	Equator Africa	3.83	3.76	-0.07(-1.8%)	5.74	1.91(49.9%)	5.72	1.89(49.3%)	5.27	1.44(37.6%)	
Subarctic Areas and Tibet	NA Subarctic	0.32	0.14	-0.18(-56.3%)	0.71	0.39(121.9%)	0.51	0.19(59.4%)	0.47	0.15(46.9%)	
	Eurasian Subarctic	0.33	0.12	-0.21(-63.6%)	0.87	0.54(163.6%)	0.65	0.32(97.0%)	0.60	0.27(81.8%)	
	Tibet	0.64	0.54	-0.10(-15.6%)	1.36	0.72(112.5%)	0.81	0.17(26.6%)	0.75	0.11(17.2%)	
Global		1.18	1.00	-0.18(-15.3%)	2.44	1.26(110.8%)	2.31	1.13(95.8%)	2.12	0.94(79.7%)	

Note: the numbers in parentheses are relative biases



555

Figure 13. The 1982-2007 average gross primary production difference (a) NIPSN-OBS, (b) NIPSN-SSiB4, (c) SSiB5-NIPSN, and leaf area index difference (d) NIPSN- OBS, (e) NIPSN- SSiB4, (f) SSiB5- NIPSN

Note: NIPSN is N limitation on photosynthesis ($V_{c, max}$) only.

560 We imposed N limitation on several processes. Among them, Exp. NIPSN shows the largest impact. The results from Exp. NIPSN, which apply Eq. (6) to scale down the $V_{c,max}$, are discussed here. Please note, the differences between Exp. SSiB5 and Exp. NIPSN show the effects due to another two N limitation processes (Eqs. 10 and 13). Exp. NIPSN has a lower global GPP bias ($128.52 \text{ g C m}^{-2} \text{ yr}^{-1}$) compared to FLUXNET-MTE estimates than Exp. SSiB4 does ($219.50 \text{ g C m}^{-2} \text{ yr}^{-1}$) (Fig. 13, Table 6), but it is larger than Exp. SSiB5, in which the bias is $79 \text{ g C m}^{-2} \text{ yr}^{-1}$ (Table 6). In addition, Exp. NIPSN has a global LAI bias of 1.13 (Fig. 13, Table 7), which is also lower than the LAI bias in Exp. SSiB4 (1.26), but higher than Exp. SSiB5 (0.94). The largest reductions in the magnitude of the LAI bias are in North America, Eurasian continents, and tropical Savanna regions in South America and Africa (Figs. 13b and 13e). That said, the N limitation on photosynthesis plays a dominant role, contributing to about 65%/41% of the improvement for the GPP/LAI simulations in Exp. SSiB5, respectively. Adjusting $V_{c,max}$ is the most direct and process-based approach based on physiology and yields the largest impact. But N limitation on the other

570 two processes is still substantial. The N limitations on respiration and phenology have the most impact in tropical forest and savanna regions (Figs. 13c and 13f). For GPP, they also reduce the positive bias over boreal regions and the negative bias in the polar regions.



5 Discussion and Conclusions

575 This study presents improvements in modelling the C cycle by introducing plant N processes into the
SSiB5/TRIFFID/DayCent-SOM, using DayCent-SOM to obtain the amount of N available to plants and plant soil N uptake.
The approach presented in this study can also be applied to other models with similar physical and biological principles. The
new C-N coupling framework allows us to use dynamic C/N ratios to represent plant resistance and self-adjustment, which
allow adaptations in the stoichiometry of C and N. Since these processes can increase nutrient use efficiency and reduce the
580 impact of N limitation through N remobilization and resorption, N-limit effect would not linearly nor instantaneously respond
to available N content. A linear relationship between N limitation factor and available N is valid only when N availability is
not sufficient for the minimum N demand for new growth. This is an advantage of our approach. That said, with the new model
structure, N impacts on GPP are predicted directly but not linearly with leaf N content, which is affected by the state of plant
growth, autotrophic respiration, and plant phenology.

585 By comparing site-level results from SSiB4 and SSiB5 to FLUXNET GPP and surface heat fluxes from twelve sites with
representative biome types and climate zones, we gained confidence in the ability of the new N processes to enhance global
model performance. We also evaluated the model performance against global satellite product data sets for GPP and LAI. In
general, with the new plant C-N coupling framework, SSiB5/TRIFFID/DayCent-SOM produces significantly less absolute
bias for GPP and LAI than the baseline version of SSiB4/TRIFFID (without N processes), a global decrease of the bias in GPP
590 and LAI by 16.3% and 27.1%, respectively. The main improvements are found in tropical Africa and the boreal forest. The
more realistic representation of dynamic C/N ratios and plant C-N framework leads to general improvements in
SSiB5/TRIFFID/DayCent-SOM's global C cycling simulations. From the perspective of plant physiology (Högberg et al.,
2017), the downregulation of the canopy photosynthetic rate based on the available mineral N for growth of plant tissues is
more reasonable than the simple and direct downregulation of GPP or NPP. In fact, we have conducted a test to directly
595 downscale GPP and NPP, and our simulation results (not shown) support this viewpoint. This coupled model can better
reproduce observed state variables and their emergent properties (such as GPP, NPP, LAI, and respiration). Despite the general
improvement globally, the GPP simulation in the temperate East Asian mixed forest-grassland regions seems to get worse with
SSiB5 compared to SSiB4. In some regions, such as the Amazon, while the SSiB4 produced lower GPP than observations, the
imposed N limitation in SSiB5 would further increase the bias in the regions. This mismatch is a common issue reported in a
600 number of publications (Anav et al., 2015; Liu et al., 2019; Piao et al., 2013). Further investigations are necessary.

Recently, the important influence of phosphorus availability on the terrestrial ecosystem carbon uptake has been increasingly
realized. The recently initiated ecosystem-scale manipulation experiments in phosphorus-poor environments (Fleischer et al.,
2019) call for the need for new phosphorus enabled LSMs to keep track of these actions (Goll et al., 2017; Reed et al., 2015).
We plan to incorporate other plant processes, such as plant/soil phosphorus processes, to further improve performance of the
605 model in the future.



Data availability. The evaluation/reference data sets from model data discussed in this paper are archived at <https://doi.org/10.5281/zenodo.7196869>

610

Code availability. The source code of biophysical-ecosystem-biogeochemical model, SSiB version5/TRIFFID/DayCent-SOM is archived at <https://doi.org/10.5281/zenodo.7297108>

Author contributions. ZX, YX, MH, and YL designed the coupling strategy between SSiB4/TRIFFID and DayCent-SOM. ZX
615 conducted the simulation with suggestions from YX, WG, and WP. ZX, YX, and MH drafted the text and ZX made the figures.
All authors (ZX, YX, WG, MH, YL and WP) have contributed to the analysis and the text.

Competing interests. The authors declare that they have no conflict of interest.

620 *Acknowledgments* This study is supported by the National Science Foundation, Division of Atmospheric and Geospace
Sciences (Grant No. AGS-1419526, AGS-1849654), and the Fundamental Research Funds for the Central Universities (Grant
No. 14380172). The authors acknowledge the use of the Cheyenne supercomputer (<https://doi.org/10.5065/D6RX99HX>,
Computational and Information Systems Laboratory, 2019), provided by NCAR CISL, for providing HPC resources.



625 References

- Aber, J. D., Goodale, C. L., Ollinger, S. V., Smith, M.-L., Magill, A. H., Martin, M. E., Hallett, R. A., and Stoddard, J. L.: Is nitrogen deposition altering the nitrogen status of northeastern forests?, *Bioscience*, 53, 375–389, [https://doi.org/10.1641/0006-3568\(2003\)053\[0375:INDATN\]2.0.CO;2](https://doi.org/10.1641/0006-3568(2003)053[0375:INDATN]2.0.CO;2), 2003.
- Aerts, R.: Nutrient Resorption from Senescing Leaves of Perennials: Are there General Patterns?, *J. Ecol.*, 84, 597, <https://doi.org/10.2307/2261481>, 1996.
- 630 Aerts, R. and Berendse, F.: The effect of increased nutrient availability on vegetation dynamics in wet heathlands, *Vegetatio*, 76, 63–69, <https://doi.org/10.1007/BF00047389>, 1988.
- Ali, A. A., Xu, C., Rogers, A., McDowell, N. G., Medlyn, B. E., Fisher, R. A., Wullschlegel, S. D., Reich, P. B., Vrugt, J. A., Bauerle, W. L., Santiago, L. S., and Wilson, C. J.: Global-scale environmental control of plant photosynthetic capacity, *Ecol. Appl.*, 25, 2349–2365, <https://doi.org/10.1890/14-2111.1>, 2015.
- 635 Anav, A., Friedlingstein, P., Beer, C., Ciais, P., Harper, A., Jones, C., Murray-Tortarolo, G., Papale, D., Parazoo, N. C., Peylin, P., Wiltshire, A., and Zhao, M.: Spatiotemporal patterns of terrestrial gross primary production: A review, *Rev. Geophys.*, 53, 785–818, <https://doi.org/10.1002/2015RG000483>, 2015.
- Arora, V. K., Katavouta, A., Williams, R. G., Jones, C. D., Brovkin, V., Friedlingstein, P., Schwinger, J., Bopp, L., Boucher, O., Cadule, P., and Chamberlain, M. A.: Carbon – concentration and carbon – climate feedbacks in CMIP6 models and their comparison to CMIP5 models, 4173–4222, 2020.
- 640 Asaadi, A., Arora, V. K., and Arora, V. K.: Implementation of nitrogen cycle in the CLASSIC land model, *Biogeosciences*, 18, <https://doi.org/10.5194/bg-18-669-2021>, 2021.
- Bai, X., Dippold, M. A., An, S., Wang, B., Zhang, H., and Loeppmann, S.: Extracellular enzyme activity and stoichiometry: The effect of soil microbial element limitation during leaf litter decomposition, *Ecol. Indic.*, 121, <https://doi.org/10.1016/j.ecolind.2020.107200>, 2021.
- 645 Beer, C., Reichstein, M., Tomelleri, E., Ciais, P., Jung, M., Carvalhais, N., Rodenbeck, C., Arain, M. A., Baldocchi, D., Bonan, G. B., Bondeau, A., Cescatti, A., Lasslop, G., Lindroth, A., Lomas, M., Luyssaert, S., Margolis, H., Oleson, K. W., Rouspard, O., Veenendaal, E., Viovy, N., Williams, C., Woodward, F. I., and Papale, D.: Terrestrial Gross Carbon Dioxide Uptake: Global Distribution and Covariation with Climate, *Science (80-.)*, 329, 834–838, <https://doi.org/10.1126/science.1184984>, 2010.
- 650 Best, M. J., Pryor, M., Clark, D. B., Rooney, G. G., Essery, R. . L. H., Ménard, C. B., Edwards, J. M., Hendry, M. A., Porson, A., Gedney, N., Mercado, L. M., Sitch, S., Blyth, E., Boucher, O., Cox, P. M., Grimmond, C. S. B., and Harding, R. J.: The Joint UK Land Environment Simulator (JULES), model description – Part 1: Energy and water fluxes, *Geosci. Model Dev.*, 4, 677–699, <https://doi.org/10.5194/gmd-4-677-2011>, 2011.
- 655 Bonan, G. B.: Forests and Climate Change : Climate Benefits of Forests, *Science (80-.)*, 320, 1444–1449, 2008.



- Bonan, G. B., Hartman, M. D., Parton, W. J., and Wieder, W. R.: Evaluating litter decomposition in earth system models with long-term litterbag experiments: An example using the Community Land Model version 4 (CLM4), *Glob. Chang. Biol.*, 19, 957–974, <https://doi.org/10.1111/gcb.12031>, 2013.
- 660 Chang, Y., Zhong, Q., Yang, H., Xu, C., Hua, W., and Li, B.: Patterns and driving factors of leaf C, N, and P stoichiometry in two forest types with different stand ages in a mid-subtropical zone, *For. Ecosyst.*, 9, <https://doi.org/10.1016/j.fecs.2022.100005>, 2022.
- Chen, X. and Chen, H. Y. H.: Plant mixture balances terrestrial ecosystem C:N:P stoichiometry, *Nat. Commun.*, 12, <https://doi.org/10.1038/s41467-021-24889-w>, 2021.
- 665 Clark, D. B., Mercado, L. M., Sitch, S., Jones, C. D., Gedney, N., Best, M. J., Pryor, M., Rooney, G. G., Essery, R. L. H., Blyth, E., Boucher, O., Harding, R. J., Huntingford, C., and Cox, P. M.: The Joint UK Land Environment Simulator (JULES), model description – Part 2: Carbon fluxes and vegetation dynamics, *Geosci. Model Dev.*, 4, 701–722, <https://doi.org/10.5194/gmd-4-701-2011>, 2011.
- Clarkson, D. T. and Hanson, J. B.: The Mineral Nutrition of Higher Plants, *Annu. Rev. Plant Physiol.*, 31, 239–298, <https://doi.org/10.1146/annurev.pp.31.060180.001323>, 1980.
- 670 Collatz, G. J., Ball, J. T., Grivet, C., and Berry, J. A.: Physiological and environmental regulation of stomatal conductance, photosynthesis and transpiration: a model that includes a laminar boundary layer, *Agric. For. Meteorol.*, 54, 107–136, [https://doi.org/10.1016/0168-1923\(91\)90002-8](https://doi.org/10.1016/0168-1923(91)90002-8), 1991.
- Cox, P. M.: Description of the “TRIFFID” Dynamic Global Vegetation Model, Hadley Cent. Tech. Note-24, 2001.
- 675 Dan, L., Yang, X., Yang, F., Peng, J., Li, Y., Gao, D., Ji, J., And Huang, M.: Integration of nitrogen dynamics into the land surface model AVIM. Part 2: baseline data and variation of carbon and nitrogen fluxes in China, *Atmos. Ocean. Sci. Lett.*, 13, <https://doi.org/10.1080/16742834.2020.1819145>, 2020.
- Davies-Barnard, T., Meyerholt, J., Zaehle, S., Friedlingstein, P., Brovkin, V., Fan, Y., Fisher, R. A., Jones, C. D., Lee, H., Peano, D., Smith, B., Wärlind, D., and Wiltshire, A. J.: Nitrogen cycling in CMIP6 land surface models: Progress and
680 limitations, *Biogeosciences*, 17, 5129–5148, <https://doi.org/10.5194/bg-17-5129-2020>, 2020.
- Ding, D., Arif, M., Liu, M., Li, J., Hu, X., Geng, Q., Yin, F., and Li, C.: Plant-soil interactions and C:N:P stoichiometric homeostasis of plant organs in riparian plantation, *Front. Plant Sci.*, 13, <https://doi.org/10.3389/fpls.2022.979023>, 2022.
- Dorman, J. L. and Sellers, P. J.: A global climatology of albedo, roughness length and stomatal resistance for atmospheric general circulation models as represented by the Simple Biosphere Model (SiB), *J. Appl. Meteorol.*, 28, 833–855,
685 [https://doi.org/10.1175/1520-0450\(1989\)028<0833:AGCOAR>2.0.CO;2](https://doi.org/10.1175/1520-0450(1989)028<0833:AGCOAR>2.0.CO;2), 1989.
- Drewniak, B. and Gonzalez-Meler, M.: Earth System Model Needs for Including the Interactive Representation of Nitrogen Deposition and Drought Effects on Forested Ecosystems, *Forests*, 8, 267, <https://doi.org/10.3390/f8080267>, 2017.
- Du, E., Terrer, C., Pellegrini, A. F. A., Ahlström, A., van Lissa, C. J., Zhao, X., Xia, N., Wu, X., and Jackson, R. B.: Global patterns of terrestrial nitrogen and phosphorus limitation, *Nat. Geosci.*, 13, 221–226, <https://doi.org/10.1038/s41561-019-0530-4>,
690 2020.



- Evans, J. R.: Photosynthesis and nitrogen relationships in leaves of C_3 plants, *Oecologia*, 78, 9–19, <https://doi.org/10.1007/BF00377192>, 1989.
- Eyring, V., Bony, S., Meehl, G. A., Senior, C. A., Stevens, B., Stouffer, R. J., and Taylor, K. E.: Overview of the Coupled Model Intercomparison Project Phase 6 (CMIP6) experimental design and organization, *Geosci. Model Dev.*, 9, 1937–1958, <https://doi.org/10.5194/gmd-9-1937-2016>, 2016.
- 695 Farquhar, G. D., von Caemmerer, S., and Berry, J. A.: A biochemical model of photosynthetic CO_2 assimilation in leaves of C_3 species, *Planta*, 149, 78–90, <https://doi.org/10.1007/BF00386231>, 1980.
- Fisher, J. B., Sitch, S., Malhi, Y., Fisher, R. A., Huntingford, C., and Tan, S.-Y.: Carbon cost of plant nitrogen acquisition: A mechanistic, globally applicable model of plant nitrogen uptake, retranslocation, and fixation, *Global Biogeochem. Cycles*, 24, n/a-n/a, <https://doi.org/10.1029/2009gb003621>, 2010.
- 700 Fleischer, K., Rammig, A., De Kauwe, M. G., Walker, A. P., Domingues, T. F., Fuchslueger, L., Garcia, S., Goll, D. S., Grandis, A., Jiang, M., Haverd, V., Hofhansl, F., Holm, J. A., Kruijt, B., Leung, F., Medlyn, B. E., Mercado, L. M., Norby, R. J., Pak, B., von Randow, C., Quesada, C. A., Schaap, K. J., Valverde-Barrantes, O. J., Wang, Y. P., Yang, X., Zaehle, S., Zhu, Q., and Lapola, D. M.: Amazon forest response to CO_2 fertilization dependent on plant phosphorus acquisition, *Nat. Geosci.*, 12, <https://doi.org/10.1038/s41561-019-0404-9>, 2019.
- 705 Foley, J. A., Levis, S., Prentice, I. C., Pollard, D., and Thompson, S. L.: Coupling dynamic models of climate and vegetation, *Glob. Chang. Biol.*, 4, 561–579, <https://doi.org/10.1046/j.1365-2486.1998.t01-1-00168.x>, 1998.
- Friedlingstein, P., Cox, P., Betts, R., Bopp, L., von Bloh, W., Brovkin, V., Cadule, P., Doney, S., Eby, M., Fung, I., Bala, G., John, J., Jones, C., Joos, F., Kato, T., Kawamiya, M., Knorr, W., Lindsay, K., Matthews, H. D., Raddatz, T., Rayner, P., Reick, C., Roeckner, E., Schnitzler, K.-G., Schnur, R., Strassmann, K., Weaver, A. J., Yoshikawa, C., and Zeng, N.: Climate–Carbon Cycle Feedback Analysis: Results from the C_4 MIP Model Intercomparison, *J. Clim.*, 19, 3337–3353, <https://doi.org/10.1175/JCLI3800.1>, 2006.
- Gerber, S., Hedin, L. O., Oppenheimer, M., Pacala, S. W., and Shevliakova, E.: Nitrogen cycling and feedbacks in a global dynamic land model, *Global Biogeochem. Cycles*, 24, 1–15, <https://doi.org/10.1029/2008GB003336>, 2010.
- 715 Ghimire, B., Riley, W. J., Koven, C. D., Mu, M., and Randerson, J. T.: Representing leaf and root physiological traits in CLM improves global carbon and nitrogen cycling predictions, *J. Adv. Model. Earth Syst.*, 8, 598–613, <https://doi.org/10.1002/2015MS000538>, 2016.
- Goll, D. S., Winkler, A. J., Raddatz, T., Dong, N., Colin Prentice, I., Ciais, P., and Brovkin, V.: Carbon-nitrogen interactions in idealized simulations with JSBACH (version 3.10), *Geosci. Model Dev.*, 10, 2009–2030, <https://doi.org/10.5194/gmd-10-2009-2017>, 2017.
- 720 Gregory, J. M., Jones, C. D., Cadule, P., and Friedlingstein, P.: Quantifying carbon cycle feedbacks, *J. Clim.*, 22, 5232–5250, <https://doi.org/10.1175/2009JCLI2949.1>, 2009.



- Gristina, L., Scalenghe, R., García-Díaz, A., Matranga, M. G., Ferraro, V., Guaitoli, F., and Novara, A.: Soil organic carbon stocks under recommended management practices in different soils of semiarid vineyards, *L. Degrad. Dev.*, 31, 725 <https://doi.org/10.1002/ldr.3339>, 2020.
- Del Grosso, S. J., Parton, W. J., Mosier, A. R., Ojima, D. S., Kulmala, A. E., and Phongpan, S.: General model for N₂O and N₂ gas emissions from soils due to denitrification, *Global Biogeochem. Cycles*, 14, 1045–1060, <https://doi.org/10.1029/1999GB001225>, 2000.
- Harper, A. B., Cox, P. M., Friedlingstein, P., Wiltshire, A. J., Jones, C. D., Sitch, S., Mercado, L. M., Groenendijk, M., 730 Robertson, E., Kattge, J., Bönisch, G., Atkin, O. K., Bahn, M., Cornelissen, J., Niinemets, Ü., Onipchenko, V., Peñuelas, J., Poorter, L., Reich, P. B., Soudzilovskaia, N. A., and Van Bodegom, P.: Improved representation of plant functional types and physiology in the Joint UK Land Environment Simulator (JULES v4.2) using plant trait information, *Geosci. Model Dev.*, 9, 2415–2440, <https://doi.org/10.5194/gmd-9-2415-2016>, 2016.
- Heikkinen, J., Keskinen, R., Regina, K., Honkanen, H., and Nuutinen, V.: Estimation of carbon stocks in boreal cropland soils 735 - methodological considerations, *Eur. J. Soil Sci.*, 72, <https://doi.org/10.1111/ejss.13033>, 2021.
- Herbert, D. A. and Fownes, J. H.: Phosphorus limitation of forest leaf area and net primary production on a highly weathered soil, *Ecosystems*, 29, 242–25, <https://doi.org/10.1007/BF02186049>, 1999.
- Högberg, P., Näsholm, T., Franklin, O., and Högberg, M. N.: Tamm Review: On the nature of the nitrogen limitation to plant growth in Fennoscandian boreal forests, <https://doi.org/10.1016/j.foreco.2017.04.045>, 1 November 2017.
- Hu, S., Chapin, F. S., Firestone, M. K., Field, C. B., and Chiariello, N. R.: Nitrogen limitation of microbial decomposition in 740 a grassland under elevated CO₂, *Nature*, 409, 188–191, <https://doi.org/10.1038/35051576>, 2001.
- Huang, H., Xue, Y., Li, F., and Liu, Y.: Modeling long-term fire impact on ecosystem characteristics and surface energy using a process-based vegetation-fire model SSiB4/TRIFFID-Fire v1.0, *Geosci. Model Dev. Discuss.*, 1–41, <https://doi.org/10.5194/gmd-2020-122>, 2020.
- Jiang, L., Lu, L., Jiang, L., Qi, Y., and Yang, A.: Impact of a detailed urban parameterization on modeling the urban heat island 745 in Beijing using TEB-RAMS, *Adv. Meteorol.*, 2014, <https://doi.org/10.1155/2014/602528>, 2014.
- Jung, M., Reichstein, M., and Bondeau, A.: Towards global empirical upscaling of FLUXNET eddy covariance observations: Validation of a model tree ensemble approach using a biosphere model, *Biogeosciences*, 6, 2001–2013, <https://doi.org/10.5194/bg-6-2001-2009>, 2009.
- 750 Jung, M., Reichstein, M., Margolis, H. A., Cescatti, A., Richardson, A. D., Arain, M. A., Arneth, A., Bernhofer, C., Bonal, D., Chen, J., Gianelle, D., Gobron, N., Kiely, G., Kutsch, W., Lasslop, G., Law, B. E., Lindroth, A., Merbold, L., Montagnani, L., Moors, E. J., Papale, D., Sottocornola, M., Vaccari, F., and Williams, C.: Global patterns of land-atmosphere fluxes of carbon dioxide, latent heat, and sensible heat derived from eddy covariance, satellite, and meteorological observations, *J. Geophys. Res. Biogeosciences*, 116, <https://doi.org/10.1029/2010JG001566>, 2011.
- 755 Kaiser, C., Franklin, O., Dieckmann, U., and Richter, A.: Microbial community dynamics alleviate stoichiometric constraints during litter decay, *Ecol. Lett.*, 17, <https://doi.org/10.1111/ele.12269>, 2014.



- Kattge, J., Knorr, W., Raddatz, T., and Wirth, C.: Quantifying photosynthetic capacity and its relationship to leaf nitrogen content for global-scale terrestrial biosphere models, *Glob. Chang. Biol.*, 15, 976–991, <https://doi.org/10.1111/j.1365-2486.2008.01744.x>, 2009.
- 760 Kolb, K. J. and Evans, R. D.: Implications of leaf nitrogen recycling on the nitrogen isotope composition of deciduous plant tissues, *New Phytol.*, 156, 57–64, <https://doi.org/10.1046/j.1469-8137.2002.00490.x>, 2002.
- Krinner, G., Viovy, N., de Noblet-Ducoudré, N., Ogée, J., Polcher, J., Friedlingstein, P., Ciais, P., Sitch, S., and Prentice, I. C.: A dynamic global vegetation model for studies of the coupled atmosphere-biosphere system, *Global Biogeochem. Cycles*, 19, 1–33, <https://doi.org/10.1029/2003GB002199>, 2005.
- 765 Lawrence, D. M., Fisher, R. A., Koven, C. D., Oleson, K. W., Swenson, S. C., Bonan, G., Collier, N., Ghimire, B., van Kampenhout, L., Kennedy, D., Kluzek, E., Lawrence, P. J., Li, F., Li, H., Lombardozzi, D., Riley, W. J., Sacks, W. J., Shi, M., Vertenstein, M., Wieder, W. R., Xu, C., Ali, A. A., Badger, A. M., Bisht, G., van den Broeke, M., Brunke, M. A., Burns, S. P., Buzan, J., Clark, M., Craig, A., Dahlin, K., Drewniak, B., Fisher, J. B., Flanner, M., Fox, A. M., Gentine, P., Hoffman, F., Keppel-Aleks, G., Knox, R., Kumar, S., Lenaerts, J., Leung, L. R., Lipscomb, W. H., Lu, Y., Pandey, A., Pelletier, J. D., Perket,
770 J., Randerson, J. T., Ricciuto, D. M., Sanderson, B. M., Slater, A., Subin, Z. M., Tang, J., Thomas, R. Q., Val Martin, M., and Zeng, X.: The Community Land Model Version 5: Description of New Features, Benchmarking, and Impact of Forcing Uncertainty, *J. Adv. Model. Earth Syst.*, 11, 4245–4287, <https://doi.org/10.1029/2018MS001583>, 2019.
- LeBauer, D. S. and Treseder, K. K.: NITROGEN LIMITATION OF NET PRIMARY PRODUCTIVITY IN TERRESTRIAL ECOSYSTEMS IS GLOBALLY DISTRIBUTED, *Ecology*, 89, 371–379, <https://doi.org/10.1890/06-2057.1>, 2008.
- 775 Lin, Y., Lai, Y., Tang, S., Qin, Z., Liu, J., Kang, F., and Kuang, Y.: Climatic and edaphic variables determine leaf C, N, P stoichiometry of deciduous *Quercus* species, *Plant Soil*, 474, <https://doi.org/10.1007/s11104-022-05342-3>, 2022.
- Liu, Y., Xue, Y., Macdonald, G., Cox, P., and Zhang, Z.: Global vegetation variability and its response to elevated CO₂, global warming, and climate variability - A study using the offline SSiB4/TRIFFID model and satellite data, *Earth Syst. Dyn.*, 10, 9–29, <https://doi.org/10.5194/esd-10-9-2019>, 2019.
- 780 Liu, Y., Xue, Y., Li, Q., Lettenmaier, D., and Zhao, P.: Investigation of the Variability of Near-Surface Temperature Anomaly and Its Causes Over the Tibetan Plateau, *J. Geophys. Res. Atmos.*, 125, <https://doi.org/10.1029/2020JD032800>, 2020.
- Ma, H.-Y., Mechoso, C. R., Xue, Y., Xiao, H., Neelin, J. D., and Ji, X.: On the connection between continental-scale land surface processes and the tropical climate in a coupled ocean-atmosphere-land system, *J. Clim.*, 26, 9006–9025, <https://doi.org/10.1175/JCLI-D-12-00819.1>, 2013.
- 785 MacDonald, J. A., Dise, N. B., Matzner, E., Armbruster, M., Gundersen, P., and Forsius, M.: Nitrogen input together with ecosystem nitrogen enrichment predict nitrate leaching from European forests, *Glob. Chang. Biol.*, 8, 1028–1033, <https://doi.org/10.1046/j.1365-2486.2002.00532.x>, 2002.
- Makino, A. and Osmond, B.: Effects of Nitrogen Nutrition on Nitrogen Partitioning between Chloroplasts and Mitochondria in Pea and Wheat, *Plant Physiol.*, 96, 355–362, <https://doi.org/10.1104/pp.96.2.355>, 1991.



- 790 Marmann, P., Wendler, R., Millard, P., and Heilmeyer, H.: Nitrogen storage and remobilization in ash (*Fraxinus excelsior*)
under field and laboratory conditions, *Trees - Struct. Funct.*, 11, 298–305, <https://doi.org/10.1007/s004680050088>, 1997.
- Matson, P., Lohse, K. A., and Hall, S. J.: The Globalization of Nitrogen Deposition: Consequences for Terrestrial Ecosystems,
AMBIO A J. Hum. Environ., 31, 113–119, <https://doi.org/10.1579/0044-7447-31.2.113>, 2002.
- May, J. D. and Killingbeck, K. T.: Effects of preventing nutrient resorption on plant fitness and foliar nutrient dynamics,
795 *Ecology*, 73, 1868–1878, <https://doi.org/10.2307/1940038>, 1992.
- McDowell, N., Pockman, W. T., Allen, C. D., Breshears, D. D., Cobb, N., Kolb, T., Plaut, J., Sperry, J., West, A., Williams,
D. G., Williams, D. G., and Yezpez, E. A.: Mechanisms of plant survival and mortality during drought: Why do some plants
survive while others succumb to drought?, *New Phytol.*, 178, 719–739, <https://doi.org/10.1111/j.1469-8137.2008.02436.x>,
2008.
- 800 McGroddy, M. E., Daufresne, T., and Hedin, L. O.: Scaling of C:N:P stoichiometry in forests worldwide: Implications of
terrestrial redfield-type ratios, <https://doi.org/10.1890/03-0351>, 2004.
- Meyer-Grünefeldt, M., Calvo, L., Marcos, E., Von Oheimb, G., and Härdtle, W.: Impacts of drought and nitrogen addition on
Calluna heathlands differ with plant life-history stage, *J. Ecol.*, 103, 1141–1152, <https://doi.org/10.1111/1365-2745.12446>,
2015.
- 805 Millard, P.: Measurement of the remobilization of nitrogen for spring leaf growth of trees under field conditions, *Tree Physiol.*,
14, 1049–1054, <https://doi.org/10.1093/treephys/14.7-8-9.1049>, 1994.
- Morgan, J. B. and Connolly, E. L.: Plant - Soil Interactions : Nutrient Uptake, *Nat. Educ. Knowl.*, 4, 2013.
- Mueller, P., Ladiges, N., Jack, A., Schmieidl, G., Kutzbach, L., Jensen, K., and Nolte, S.: Assessing the long-term carbon-
sequestration potential of the semi-natural salt marshes in the European Wadden Sea, *Ecosphere*, 10,
810 <https://doi.org/10.1002/ecs2.2556>, 2019.
- Murray-Tortarolo, G., Anav, A., Friedlingstein, P., Sitch, S., Piao, S., Zhu, Z., Poulter, B., Zaehle, S., Ahlström, A., Lomas,
M., Viovy, N., and Zeng, N.: Evaluation of land surface models in reproducing satellite-derived LAI over the high-latitude
northern hemisphere. Part I: Uncoupled DGVMs, *Remote Sens.*, 5, 4819–4838, <https://doi.org/10.3390/rs5104819>, 2013.
- Neilsen, D., Millard, P., Neilsen, G. H., and Hogue, E. J.: Sources of N for leaf growth in a high-density apple (*Malus domestica*)
815 orchard irrigated with ammonium nitrate solution, *Tree Physiol.*, 17, 733–739, <https://doi.org/10.1093/treephys/17.11.733>,
1997.
- Niu, G. Y., Fang, Y. H., Chang, L. L., Jin, J., Yuan, H., and Zeng, X.: Enhancing the Noah-MP Ecosystem Response to
Droughts With an Explicit Representation of Plant Water Storage Supplied by Dynamic Root Water Uptake, *J. Adv. Model.*
Earth Syst., 12, <https://doi.org/10.1029/2020MS002062>, 2020.
- 820 Oleson, K. W., Lawrence, D. M., Bonan, G. B., Drewniak, B., Huang, M., Charles, D., Levis, S., Li, F., Riley, W. J., Zachary,
M., Swenson, S. C., Thornton, P. E., Bozbiyik, A., Fisher, R., Heald, C. L., Kluzek, E., Lamarque, F., Lawrence, P. J., Leung,
L. R., Muszala, S., Ricciuto, D. M., and Sacks, W.: Technical description of version 4.5 of the Community Land Model (CLM),



- NCAR Technical Note NCAR/TN-503+STR, Natl. Cent. Atmos. Res. Boulder, CO, 420pp, <https://doi.org/DOI:10.5065/D6RR1W7M>, 2013.
- 825 Oliveira, D. C. de, Oliveira, D. M. da S., Freitas, R. de C. A. de, Barreto, M. S., Almeida, R. E. M. de, Batista, R. B., and Cerri, C. E. P.: Depth assessed and up-scaling of single case studies might overestimate the role of C sequestration by pastures in the commitments of Brazil's low-carbon agriculture plan, *Carbon Manag.*, 12, <https://doi.org/10.1080/17583004.2021.1977390>, 2021.
- Pan, Y., Liu, Y., Wentworth, G. R., Zhang, L., Zhao, Y., Li, Y., Liu, X., Du, E., Fang, Y., Xiao, H., Ma, H., and Wang, Y.: Letter to the editor: Critical assessments of the current state of scientific knowledge, terminology, and research needs concerning the ecological effects of elevated atmospheric nitrogen deposition in China, *Atmos. Environ.*, 153, 109–116, <https://doi.org/10.1016/j.atmosenv.2017.01.015>, 2017.
- 830 Parton, W., Silver, W. L., Burke, I. C., Grassens, L., Harmon, M. E., Currie, W. S., King, J. Y., Adair, E. C., Brandt, L. A., Hart, S. C., and Fasth, B.: Global-scale similarities in nitrogen release patterns during long-term decomposition, *Science (80-.)*, 315, 361–364, <https://doi.org/10.1126/science.1134853>, 2007.
- 835 Parton, W. J., Scurlock, J. M. O., Ojima, D. S., Gilmanov, T. G., Scholes, R. J., Schimel, D. S., Kirchner, T., Menaut, J.-C., Seastedt, T., Garcia Moya, E., Kamnalrut, A., and Kinyamario, J. I.: Observations and modeling of biomass and soil organic matter dynamics for the grassland biome worldwide, *Global Biogeochem. Cycles*, 7, 785–809, <https://doi.org/10.1029/93GB02042>, 1993.
- 840 Parton, W. J., Ojima, D. S., Cole, C. V., and Schimel, D. S.: A general model for soil organic matter dynamics: sensitivity to litter chemistry, texture and management, *Quant. Model. soil Form. Process. Proc. Symp. Minneapolis*, 1992, 1994.
- Parton, W. J., Hartman, M., Ojima, D., and Schimel, D.: DAYCENT and its land surface submodel: description and testing, *Glob. Planet. Change*, 19, 35–48, [https://doi.org/10.1016/S0921-8181\(98\)00040-X](https://doi.org/10.1016/S0921-8181(98)00040-X), 1998.
- 845 Parton, W. J., Hanson, P. J., Swanston, C., Torn, M., Trumbore, S. E., Riley, W., and Kelly, R.: ForCent model development and testing using the Enriched Background Isotope Study experiment, *J. Geophys. Res. Biogeosciences*, 115, 1–15, <https://doi.org/10.1029/2009JG001193>, 2010.
- Pastorello, G., Trotta, C., Canfora, E., Chu, H., Christianson, D., Cheah, Y. W., Poindexter, C., Chen, J., Elbashandy, A., Humphrey, M., Isaac, P., Polidori, D., Ribeca, A., van Ingen, C., Zhang, L., Amiro, B., Ammann, C., Arain, M. A., Ardö, J., Arkebauer, T., Arndt, S. K., Arriga, N., Aubinet, M., Aurela, M., Baldocchi, D., Barr, A., Beamesderfer, E., Marchesini, L. B.,
- 850 Bergeron, O., Beringer, J., Bernhofer, C., Berveiller, D., Billesbach, D., Black, T. A., Blanken, P. D., Bohrer, G., Boike, J., Bolstad, P. V., Bonal, D., Bonnefond, J. M., Bowling, D. R., Bracho, R., Brodeur, J., Brümmer, C., Buchmann, N., Burban, B., Burns, S. P., Buysse, P., Cale, P., Cavagna, M., Cellier, P., Chen, S., Chini, I., Christensen, T. R., Cleverly, J., Collalti, A., Consalvo, C., Cook, B. D., Cook, D., Coursolle, C., Cremonese, E., Curtis, P. S., D'Andrea, E., da Rocha, H., Dai, X., Davis, K. J., De Cinti, B., de Grandcourt, A., De Ligne, A., De Oliveira, R. C., Delpierre, N., Desai, A. R., Di Bella, C. M., di
- 855 Tommasi, P., Dolman, H., Domingo, F., Dong, G., Dore, S., Duce, P., Dufrêne, E., Dunn, A., Dušek, J., Eamus, D., Eichelmann, U., ElKhidir, H. A. M., Eugster, W., Ewenz, C. M., Ewers, B., Famulari, D., Fares, S., Feigenwinter, I., Feitz, A., Fensholt,



- R., Filippa, G., Fischer, M., Frank, J., Galvagno, M., Gharun, M., Gianelle, D., et al.: The FLUXNET2015 dataset and the ONEFlux processing pipeline for eddy covariance data, *Sci. data*, 7, <https://doi.org/10.1038/s41597-020-0534-3>, 2020.
- Peñuelas, J., Poulter, B., Sardans, J., Ciais, P., Van Der Velde, M., Bopp, L., Boucher, O., Godderis, Y., Hinsinger, P., Llusia, J., Nardin, E., Vicca, S., Obersteiner, M., and Janssens, I. A.: Human-induced nitrogen-phosphorus imbalances alter natural and managed ecosystems across the globe, *Nat. Commun.*, 4, <https://doi.org/10.1038/ncomms3934>, 2013.
- Piao, S., Sitch, S., Ciais, P., Friedlingstein, P., Peylin, P., Wang, X., Ahlström, A., Anav, A., Canadell, J. G., Cong, N., Zaehle, S., and Zeng, N.: Evaluation of terrestrial carbon cycle models for their response to climate variability and to CO₂ trends, *Glob. Chang. Biol.*, 19, 2117–2132, <https://doi.org/10.1111/gcb.12187>, 2013.
- Raddatz, T. J., Reick, C. H., Knorr, W., Kattge, J., Roeckner, E., Schnur, R., Schnitzler, K. G., Wetzell, P., and Jungclaus, J.: Will the tropical land biosphere dominate the climate-carbon cycle feedback during the twenty-first century?, *Clim. Dyn.*, 29, 565–574, <https://doi.org/10.1007/s00382-007-0247-8>, 2007.
- Reed, S. C., Yang, X., and Thornton, P. E.: Incorporating phosphorus cycling into global modeling efforts: A worthwhile, tractable endeavor, *New Phytol.*, 208, <https://doi.org/10.1111/nph.13521>, 2015.
- Reich, P. B., Hobbie, S. E., Lee, T., Ellsworth, D. S., West, J. B., Tilman, D., Knops, J. M. H., Naeem, S., and Trost, J.: Nitrogen limitation constrains sustainability of ecosystem response to CO₂, *Nature*, 440, 922–925, <https://doi.org/10.1038/nature04486>, 2006.
- Reich, P. B., Tjoelker, M. G., Pregitzer, K. S., Wright, I. J., Oleksyn, J., and Machado, J. L.: Scaling of respiration to nitrogen in leaves, stems and roots of higher land plants, *Ecol. Lett.*, 11, 793–801, <https://doi.org/10.1111/j.1461-0248.2008.01185.x>, 2008.
- Richardson, A. D., Anderson, R. S., Arain, M. A., Barr, A. G., Bohrer, G., Chen, G., Chen, J. M., Ciais, P., Davis, K. J., Desai, A. R., Dietze, M. C., Dragoni, D., Garrity, S. R., Gough, C. M., Grant, R., Hollinger, D. Y., Margolis, H. A., McCaughey, H., Migliavacca, M., Monson, R. K., Munger, J. W., Poulter, B., Raczka, B. M., Ricciuto, D. M., Sahoo, A. K., Schaefer, K., Tian, H., Vargas, R., Verbeeck, H., Xiao, J., and Xue, Y.: Terrestrial biosphere models need better representation of vegetation phenology: Results from the North American Carbon Program Site Synthesis, *Glob. Chang. Biol.*, 18, <https://doi.org/10.1111/j.1365-2486.2011.02562.x>, 2012.
- Rogers, A.: The use and misuse of V(c,max) in Earth System Models., *Photosynth. Res.*, 119, 15–29, <https://doi.org/10.1007/s11120-013-9818-1>, 2014.
- Sardans, J., Rivas-Ubach, A., and Peñuelas, J.: The C:N:P stoichiometry of organisms and ecosystems in a changing world: A review and perspectives, <https://doi.org/10.1016/j.ppees.2011.08.002>, 2012.
- Sellers, P. J., Mintz, Y., Sud, Y. C., and Dalcher, A.: A Simple Biosphere Model (SIB) for Use within General Circulation Models, *J. Atmos. Sci.*, 43, 505–531, [https://doi.org/10.1175/1520-0469\(1986\)043<0505:ASBMFU>2.0.CO;2](https://doi.org/10.1175/1520-0469(1986)043<0505:ASBMFU>2.0.CO;2), 1986.
- Sheffield, J., Goteti, G., and Wood, E. F.: Development of a 50-year high-resolution global dataset of meteorological forcings for land surface modeling, *J. Clim.*, 19, 3088–3111, <https://doi.org/10.1175/JCLI3790.1>, 2006.



- 890 Sitch, S., Prentice, I. C., Arneth, A., Bondeau, A., Cramer, W., Kaplan, J. O., Levis, S., Lucht, W., Sykes, M. T., Thonicke, K., and Venevsky, S.: Evaluation of ecosystem dynamics, plant geography and terrestrial carbon cycling in the LPJ dynamic global vegetation model, *Glob. Chang. Biol.*, 9, 161–185, <https://doi.org/10.1046/j.1365-2486.2003.00569.x>, 2003.
- Smith, B., Wärlind, D., Arneth, A., Hickler, T., Leadley, P., Siltberg, J., and Zaehle, S.: Implications of incorporating N cycling and N limitations on primary production in an individual-based dynamic vegetation model, *Biogeosciences*, 11, 2027–2054, 895 <https://doi.org/10.5194/bg-11-2027-2014>, 2014.
- Smith, S. V.: Stoichiometry of C:N:P Fluxes in Shallow-Water Marine Ecosystems, in: *Comparative Analyses of Ecosystems*, https://doi.org/10.1007/978-1-4612-3122-6_13, 1991.
- Stenberg, J. A. and Muola, A.: How should plant resistance to herbivores be measured?, <https://doi.org/10.3389/fpls.2017.00663>, 2017.
- 900 Sterner, R. . and Elser, J. .: *Ecological Stoichiometry: The Biology of Elements from Molecules to the Biosphere*: Robert W. Sterner, James J. Elser, Peter Vitousek, 2002.
- Sun, S. and Xue, Y.: Implementing a New Snow Scheme in Simplified Simple Biosphere Model, *Adv. Atmos. Sci.*, 18, <https://doi.org/10.1007/bf02919314>, 2001.
- Talhelm, A. F., Pregitzer, K. S., and Burton, A. J.: No evidence that chronic nitrogen additions increase photosynthesis in 905 mature sugar maple forests, *Ecol. Appl.*, 21, 2413–2424, <https://doi.org/10.1890/10-2076.1>, 2011.
- Talmy, D., Blackford, J., Hardman-Mountford, N. J., Polimene, L., Follows, M. J., and Geider, R. J.: Flexible C : N ratio enhances metabolism of large phytoplankton when resource supply is intermittent, *Biogeosciences*, 11, <https://doi.org/10.5194/bg-11-4881-2014>, 2014.
- Thomas, R. Q., Brookshire, E. N. J., and Gerber, S.: Nitrogen limitation on land: How can it occur in Earth system models?, 910 *Glob. Chang. Biol.*, 21, 1777–1793, <https://doi.org/10.1111/gcb.12813>, 2015.
- Thornely, J. H. M. and Johnson, I. R.: *Plant Growth Modelling: A Mathematical approach to Plant and Crop Physiology*, 1990.
- Thum, T., Caldararu, S., Engel, J., Kern, M., Pallandt, M., Schnur, R., Yu, L., and Zaehle, S.: A new model of the coupled carbon, nitrogen, and phosphorus cycles in the terrestrial biosphere (QUINCY v1.0; revision 1996), *Geosci. Model Dev.*, 12, <https://doi.org/10.5194/gmd-12-4781-2019>, 2019.
- 915 Vicca, S., Luysaert, S., Peñuelas, J., Campioli, M., Chapin, F. S., Ciais, P., Heinemeyer, A., Högberg, P., Kutsch, W. L., Law, B. E., Malhi, Y., Papale, D., Piao, S. L., Reichstein, M., Schulze, E. D., and Janssens, I. A.: Fertile forests produce biomass more efficiently, *Ecol. Lett.*, 15, 520–526, <https://doi.org/10.1111/j.1461-0248.2012.01775.x>, 2012.
- Vitousek, P.: Nutrient Cycling and Nutrient Use Efficiency Author (s): Peter Vitousek Source : *The American Naturalist* , Vol . 119 , No . 4 (Apr ., 1982), pp . 553-572 Published by : The University of Chicago Press for The American Society of 920 Naturalists Stable URL, 119, 553–572, 1982.
- Vitousek, P. and Howarth, R.: Nitrogen limitation on land and in the sea: How can it occur?, *Biogeochemistry*, 13, 3646–3653, <https://doi.org/10.1007/BF00002772>, 1991.



- Wang, Y. P., Law, R. M., and Pak, B.: A global model of carbon, nitrogen and phosphorus cycles for the terrestrial biosphere, *Biogeosciences*, 7, 2261–2282, <https://doi.org/10.5194/bg-7-2261-2010>, 2010.
- 925 Wiltshire, A., Burke, E., Chadburn, S., Jones, C., Cox, P., Davies-Barnard, T., Friedlingstein, P., Harper, A., Liddicoat, S., Sitch, S., and Zaehle, S.: JULES-CN: a coupled terrestrial Carbon-Nitrogen Scheme (JULES vn5.1), *Geosci. Model Dev. Discuss.*, 1–40, <https://doi.org/10.5194/gmd-2020-205>, 2020.
- Xiao, Z., Liang, S., Wang, J., Chen, P., Yin, X., Zhang, L., and Song, J.: Use of general regression neural networks for generating the GLASS leaf area index product from time-series MODIS surface reflectance, *IEEE Trans. Geosci. Remote*
- 930 *Sens.*, 52, 209–223, <https://doi.org/10.1109/TGRS.2013.2237780>, 2014.
- Xue, Y., Sellers, P. J., Kinter, J. L., and Shukla, J.: A Simplified biosphere model for global climate studies, *J. Clim.*, 4, 345–364, [https://doi.org/10.1175/1520-0442\(1991\)004<0345:ASBMFG>2.0.CO;2](https://doi.org/10.1175/1520-0442(1991)004<0345:ASBMFG>2.0.CO;2), 1991.
- Xue, Y., Zeng, F. J., and Schlosser, C. A.: SSiB and its sensitivity to soil properties-A case study using HAPEX-Mobilhy data, *Glob. Planet. Change*, 13, [https://doi.org/10.1016/0921-8181\(95\)00045-3](https://doi.org/10.1016/0921-8181(95)00045-3), 1996.
- 935 Xue, Y., Sellers, P. J., Zeng, F. J., and Schlosser, C. A.: Comments on “Use of midlatitude soil moisture and meteorological observations to validate soil moisture simulations with biosphere and bucket models,” *J. Clim.*, 10, [https://doi.org/10.1175/1520-0442\(1997\)010<0374:COUOMS>2.0.CO;2](https://doi.org/10.1175/1520-0442(1997)010<0374:COUOMS>2.0.CO;2), 1997.
- Xue, Y., Juang, H.-M. H., Li, W.-P., Prince, S., DeFries, R., Jiao, Y., and Vasic, R.: Role of land surface processes in monsoon development: East Asia and West Africa, *J. Geophys. Res. Atmos.*, 109, n/a-n/a, <https://doi.org/10.1029/2003jd003556>, 2004.
- 940 Xue, Y., De Sales, F., Vasic, R., Mechoso, C. R., Arakawa, A., and Prince, S.: Global and seasonal assessment of interactions between climate and vegetation biophysical processes: A GCM study with different land-vegetation representations, *J. Clim.*, 23, 1411–1433, <https://doi.org/10.1175/2009JCLI3054.1>, 2010.
- Xue, Y., Diallo, I., Boone, A. A., Yao, T., Zhang, Y., Zeng, X., Neelin, J. D., Lau, W. K. M., Pan, Y., Liu, Y., Pan, X., Tang, Q., Oevelen, P. J. van, Sato, T., Koo, M.-S., Materia, S., Shi, C., Yang, J., Ardilouze, C., Lin, Z., Qi, X., Nakamura, T., Saha,
- 945 S. K., Senan, R., Takaya, Y., Wang, H., Zhang, H., Zhao, M., Nayak, H. P., Chen, Q., Feng, J., Brunke, M. A., Fan, T., Hong, S., Nobre, P., Peano, D., Qin, Y., Vitart, F., Xie, S., Zhan, Y., Klocke, D., Leung, R., Li, X., Ek, M., Guo, W., Balsamo, G., Bao, Q., Chou, S. C., Rosnay, P. de, Lin, Y., Zhu, Y., Qian, Y., Zhao, P., Tang, J., Liang, X.-Z., Hong, J., Ji, D., Ji, Z., Qiu, Y., Sugimoto, S., Wang, W., Yang, K., and Yu, M.: Spring Land Temperature in Tibetan Plateau and Global-Scale Summer Precipitation: Initialization and Improved Prediction, *Bull. Am. Meteorol. Soc.*, 103, [https://doi.org/10.1175/bams-d-21-](https://doi.org/10.1175/bams-d-21-0270.1)
- 950 [0270.1](https://doi.org/10.1175/bams-d-21-0270.1), 2022.
- Xue, Y., Diallo, I., Boone, A. A., Zhang, Y., Zeng, X., Lau, W. K. M., Neelin, J. D., Yao, T., Tang, Q., Sato, T., Koo, M. S., Vitart, F., Ardilouze, C., Saha, S. K., Materia, S., Lin, Z., Takaya, Y., Yang, J., Nakamura, T., Qi, X., Qin, Y., Nobre, P., Senan, R., Wang, H., Zhang, H., Zhao, M., Nayak, H. P., Pan, Y., Pan, X., Feng, J., Shi, C., Xie, S., Brunke, M. A., Bao, Q., Bottino, M. J., Fan, T., Hong, S., Lin, Y., Peano, D., Zhan, Y., Mechoso, C. R., Ren, X., Balsamo, G., Chou, S. C., de Rosnay,
- 955 P., van Oevelen, P. J., Klocke, D., Ek, M., Li, X., Guo, W., Zhu, Y., Tang, J., Liang, X. Z., Qian, Y., and Zhao, P.: Remote effects of Tibetan Plateau spring land temperature on global subseasonal to seasonal precipitation prediction and comparison



- with effects of sea surface temperature: the GEWEX/LS4P Phase I experiment, *Clim. Dyn.*, <https://doi.org/10.1007/s00382-023-06905-5>, 2023.
- 960 Yang, S., Shi, Z., Zhang, M., Li, Y., Gao, J., Wang, X., and Liu, D.: Stoichiometry of Carbon, Nitrogen and Phosphorus in Shrub Organs Linked Closely With Mycorrhizal Strategy in Northern China, *Front. Plant Sci.*, 12, <https://doi.org/10.3389/fpls.2021.687347>, 2021.
- Yang, X., Dan, L., Yang, F., Peng, J., Li, Y., Gao, D., Ji, J., And Huang, M.: The integration of nitrogen dynamics into a land surface model. Part 1: model description and site-scale validation, *Atmos. Ocean. Sci. Lett.*, 12, <https://doi.org/10.1080/16742834.2019.1548246>, 2019.
- 965 Yu, L., Ahrens, B., Wutzler, T., Zaehle, S., and Schrupf, M.: Modeling Soil Responses to Nitrogen and Phosphorus Fertilization Along a Soil Phosphorus Stock Gradient, *Front. For. Glob. Chang.*, 3, <https://doi.org/10.3389/ffgc.2020.543112>, 2020.
- Zaehle, S., Jones, C. D., Houlton, B., Lamarque, J. F., and Robertson, E.: Nitrogen availability reduces CMIP5 projections of twenty-first-century land carbon uptake, *J. Clim.*, 28, 2494–2511, <https://doi.org/10.1175/JCLI-D-13-00776.1>, 2015.
- 970 Zhan, X., Xue, Y., and Collatz, G. J.: An analytical approach for estimating CO₂ and heat fluxes over the Amazonian region, *Ecol. Modell.*, 162, 97–117, [https://doi.org/10.1016/S0304-3800\(02\)00405-2](https://doi.org/10.1016/S0304-3800(02)00405-2), 2003.
- Zhang, C., Zeng, F., Zeng, Z., Du, H., Zhang, L., Su, L., Lu, M., and Zhang, H.: Carbon, Nitrogen and Phosphorus Stoichiometry and Its Influencing Factors in Karst Primary Forest, *Forests*, 13, <https://doi.org/10.3390/f13121990>, 2022.
- Zhang, G., Han, X., and Elser, J. J.: Rapid top-down regulation of plant C:N:P stoichiometry by grasshoppers in an Inner Mongolia grassland ecosystem, *Oecologia*, 166, <https://doi.org/10.1007/s00442-011-1904-5>, 2011.
- 975 Zhang, Z., Xue, Y., MacDonald, G., Cox, P. M., and Collatz, G. J.: Investigation of North American vegetation variability under recent climate: A study using the SSiB4/TRIFFID biophysical/dynamic vegetation model, *J. Geophys. Res.*, 120, 1300–1321, <https://doi.org/10.1002/2014JD021963>, 2015.
- Zhu, Q., Riley, W. J., Tang, J., Collier, N., Hoffman, F. M., Yang, X., and Bisht, G.: Representing Nitrogen, Phosphorus, and Carbon Interactions in the E3SM Land Model: Development and Global Benchmarking, *J. Adv. Model. Earth Syst.*, 11, <https://doi.org/10.1029/2018MS001571>, 2019.
- 980 Zhu, Z., Bi, J., Pan, Y., Ganguly, S., Anav, A., Xu, L., Samanta, A., Piao, S., Nemani, R. R., and Myneni, R. B.: Global data sets of vegetation leaf area index (LAI)_{3g} and fraction of photosynthetically active radiation (FPAR)_{3g} derived from global inventory modeling and mapping studies (GIMMS) normalized difference vegetation index (NDVI_{3G}) for the period 1981 to 985 2, *Remote Sens.*, 5, 927–948, <https://doi.org/10.3390/rs5020927>, 2013.